

Manuscript No.: hess-2015-140 (submitted on 08 Apr 2015)  
Original Title: A Global Approach to Defining Flood Seasons  
Authors: Donghoon Lee, Philip Ward and Paul Block

---

Dear Editor and Reviewers,

We would like to thank the Editor and Referee #2 for again carefully reviewing our manuscript. We have revised the manuscript accordingly and detailed these changes in the response, below. Referee comments are presented in indented text, our responses are in blue, and revised sentences are in italics. Page and line numbers are given with respect to the last revised manuscript (submitted 01 Oct 2015). The revised manuscript includes underlined (added text) and crossed out (deleted text) for easy reference.

We believe the suggestions and ensuing revisions have further improved the manuscript quality.

Yours sincerely,

Donghoon Lee

Relies to the comments of Anonymous Referee #2

Authors' replies are in blue color and revised sentences are in italics.

General Comments:

The manuscript has been revised thoroughly in the 2nd revision and it is clear from the author's responses that they did their best to incorporate all the comments of the reviewers and editor.

The clarity of the document improved considerable but there are still a few points/comments that I suggest to be considered before the final publication of the document.

I therefore recommend accepting the document with minor revisions.

Specific Comments:

Section Abstract:

P1 L3: I suggest adding in parenthesis that the high-flow season is 3 months long

The authors agree. P2 L3 has been changed to:

*Here, a novel approach to defining high-flow seasons (3-month) globally is presented by identifying temporal patterns of streamflow.*

P1 L11: I suggest detailing that the 'high-resolution high-flow seasons' are spatially high resolution (due to the gridded model)

The authors agree. P2 L11-13 has been changed to:

*These high spatial-resolution high-flow seasons and associated performance metrics allow for an improve understanding of temporal characterization of streamflow and flood potential, causation, and management.*

Section 1 Introduction:

P4 L13-14 & : Spell out PM, HS, and PAMF and put the abbreviations in parenthesis behind

The authors agree. P4 L13-17 has been changed to:

*The new measure of Peak Month (PM) and High-flow Season (HS) coupled with the model grid scale provides much higher resolution peak timings globally than previously presented (often at large basin scale or subcontinental scale.) The performance measure introduced here, which is Percentage of Annual Maximum Flow (PAMF), is also a new contribution relating the models ability to capture high flow season timing.*

Section 2:

P5 L15-16: From the paper that is cited here, it is not obvious how the model has been validated to extreme discharges (which are of key interest to this paper). Ward et al. seem to have only evaluated areas that are > 125000 km<sup>2</sup> (which are ~55 stations), which is quite different from the size of the basins/grid cells used in this study.

Additionally, it is noted here that the model has a 'strong performance', however, the paper cited shows that especially in dryer areas the model overestimated by > 50%.

I therefore suggest adding a short discussion on the reliability of the model to smaller basins and drier areas, instead of highlightening a 'strong model performance'.

The Referee's suggestion to discuss reliability at smaller basin scales is warranted, however we have not undertaken this analysis at this scale for now, instead relying on previous assessments with outputs at larger scales. We agree that further reliability analysis of extreme streamflow in smaller basins beyond Ward et al. (2013) may be insightful however have opted to delay such work. The emphasis here is really about season selection more than model performance metrics. P5 L13-16 has been changed to:

*Additionally, this model has been validated in previous studies in terms of streamflow (Van Beek et al., 2011) and terrestrial water storage (Wada et al., 2011) at stations along major rivers in the world. The model's extreme discharges are also evaluated by Ward et al. (2013) with fair to good performance at stations with large drainage area ( $\geq 125,000 \text{ km}^2$ ), corresponding to 24% of GRDC stations used in this study, excepting overestimation in several arid regions.*

Section 3:

P6 & 7 General comment on POT:

Please add a sentence/paragraph indicating that the threshold for POT can either be based on threshold that defines 'specific average number of floods' (e.g. as in Cunderlik et al. 2004) or be based on a volumetric threshold (which can either be on a year to year basis or over the entire series)(e.g. Lang et al. 1999, in which it is already stated that the POT 'requires the analysis of both , the magnitude and the time of arrival of a peak').

The authors agree in that the threshold can either be based on a specific average number of floods or on a volumetric streamflow level, however we believe that generally POT is applied to the entire time-series, rather than on a year-to-year basis. The referee mentions 'the time of arrival of peaks (Lang et al., 1999)'; we understand this as referring to the average time to reach the peak from base-flow conditions, useful for differentiating an independent flood event from serial peaks based on section 2.1 (Independence criteria) and section 2.2 (Threshold selection) from Lang et al. (1999). P6 L23-26 has been changed to:

*In contrast to the AM method, POT can capture multiple large independent floods within a single year, including the annual maximum flow, but may not capture the annual maximum flow in years in which streamflow is less than the pre-defined threshold; this threshold can either be defined based on a specific average number of floods or a specific mean exceedance level over the entire period (Cunderlik et al., 2004a; Institute of Hydrology, 1999; Lang et al., 1999).*

P6 L22: I recommend already adding the reference here to papers by Lang et al. (1999.) and the Institute of Hydrology, 1999 (mentioned at a later stage on page 8)

The authors have now added these references to the following sentence (P6 L23-26) explaining the characteristics of POT. Please see the revised text above.

P6 L23: Please remove ' , prior to a specific date ' , as this is not correct, but I presume this snippet accidentally remained there during the revisions.

The authors appreciate this catch and have removed it. Please see the revised text above.

P6 L25: replace 'miss' with 'do not capture', as the word missing invokes a drawback which is actually a feature of the method.

The authors agree with the exception of using 'may' in replace of 'do.' Please see the revised text above.

P 7 L4-8 Based on the general comment on POT above, I fail to understand why it is highlighted that the POT approach is over the entire series and not on a year-to-year basis.

Hopefully we have addressed this comment to the Referee's satisfaction in the responses above. Here, we highlight that with VBT (our proposed methodology) the threshold is applied over the entire time-series, however common volume-based technique is applied on a year-by-year basis only.

As the Section P6 L10 to P7 L 10 has been rewritten several times, it is confusing and I therefore suggest rewriting the entire paragraph incorporating the above comments.

The authors have revised the paragraph according to the above Referee comments and our responses. Please see the revised manuscript.

P 7 L10-13: As there is a thorough analysis of results of the different methods later in the paper I suggest to remove the sentence of the selection of the threshold here, as it otherwise pre-empts the detailed analysis later.

The authors agree and have removed P7 L10-13.

P 7 L 14-15: Please further elaborate, why you decide to use the month before and after (which is subjective), instead of using the adjacent months with the highest number of days above the threshold, which would be able to capture also asymmetric peak flow distribution around the PM. (This request had been already mentioned in my previous review but was not addressed by the authors yet.)

The authors apologize for not adequately addressing the Referee's previous comment. The fixed 3-month time window for the high-flow season has been designed with future work in mind, namely seasonal prediction that benefits from a uniform window for analysis at the global scale. The Referee makes a good point, however, regarding possible asymmetric distribution around the PM. It turns out from the HS perspective (3-month) though it makes little difference, since the extra months act as a buffer, and in most cases, the 3-month HS selected indeed captures the dominant 3-month period. But it is worth further investigation. Other factors also play a role in defining the HS specifically (peak duration (length of HS) and timing distribution (shape of HS), different hydrological processes affecting peak-flow behavior, etc.), and collectively may require additional analysis at a future stage. For clarity's sake at this stage, we have opted to present the method proposed. P7 L13-16 has been changed to:

*Here, the month containing the greatest number of occurrences over the specified percentage of flows across all years (1958-2000) is defined as the PM, and subsequently the HS is designated as the period containing the PM plus the month before and after the PM. Figure 2 provides an example based on seven years of synthetic streamflow with the volumetric threshold set at the top 5% of flows.*

P 7 L22: The AMF and therefore the PAMF as an evaluation measure is strongly dependent on how the year is defined (i.e. calendar year versus hydrological year). Please discuss briefly how this might affect the scores of PAMF.

The Referee highlights a good point, and indeed it is possible that AMF analyses based on calendar vs hydrological year may produce different results. This should be minimized, however, in our analysis given that our methodology is not contingent on identifying the single AMF in any 12-month period, but rather on capturing peak flows (as previously described, there could be multiple in one 12-month period or none in a 12-month period) across the time-series, and identifying the Peak Month overall. The PAMF, however, is dependent on the 12-month period selected – with the calendar month being selected here. We have not tested how the PAMF may change by using the hydrological year, however we believe that if any PAMF values change, they may improve slightly, thus using the calendar year is slightly conservative. Also, because the analysis for selecting the High-flow Season is based on selecting the single Peak Month and then sandwiching with 1 month on either side, this reduces the influence of calendar vs. hydrological year selection.

P 7 L25: Did you mean 'percentage' instead of the 'percent of time'?

Yes, thank you. P7 L25-26 has been changed to:

*Here the PAMF provides the percentage of annual maximum flows occurring in the defined HS across the evaluation period.*

P8 L12-14: Not clear what is meant here. Elaborate/further explain why this is the case.

The authors apologize for the misunderstanding. For clarification, P8 L12-14 has been changed to:

*Comparatively, techniques with a shorter time component (1-3% of annual volume) favor identifying the PM by peak timing, since the top 1-4 days of streamflow tend to be located near the peak, while techniques with longer time components (5-10% of annual volume) favor identifying the PM based on duration and peak volume, since the top 19-33 days of streamflow tend to be located near the volumetric centroid of the hydrograph, rather than the peak, if they differ.*

P8 L27-30: It is not clear if the table shows all cases or only the cases in which the PMS differ. Please explain further.

The authors apologize for the misunderstanding. Table 1 shows the cases in which the PMS differ. For clarification, the caption of the Table 1 has been changed to:

*Table 1. Cross-correlations of Peak Month (PM) at locations where the PMs differ by at least one classification technique (occurs at 61% of stations and 54% of associated grids).*

P9 L8-11: See comments on P6 L25 and P 7 L4-8 and change accordingly.

Thank you for the suggestion. P9 L8-11 has been changed to:

*This is not unexpected as the volume-based techniques are designed to capture annual peak flows on a year-by-year basis, whereas the POT and VBT record significant peaks across the full time-series, and may not capture annual peaks in some years in which that peak is small relative to all peaks throughout the available record.*

Section 4:

P 10 L 13 & 31: Based on my experience reservoirs do not exclusively result in low PMAF values (i.e. spread of the peak flow values across the months), they can also cause the opposite (concentration of the peak values into a specific month). This all depends on the operation rules!

To avoid that this strong assumption (as already mentioned by the authors in L 14) is confused with a statement of generality, I suggest that it should be made clear again in Line 31 the low PMAF this is based on an assumption and that reservoirs can also have the opposite effect.

The authors agree with the referee's comments. P10 L29-31 has been changed to:

*In this case, the effect of stations downstream of reservoirs will be minimized given their typically low average PAMF values, assuming operational rules relatively evenly distribute the annual flow across all months; however, if operational rules instead concentrate releases to a few months, PAMF values may actually be high.*

P 12 L 11: What does 'around Finland' mean? South Finland around the Baltic Sea? Please specify.

The authors apologize for the imprecise explanation. It refers to South Finland as the referee indicates. P12 L11-13 has been changed to:

*In Northern Europe, especially South Finland, this becomes much more pronounced, with large differences between PMs from observations and the model, on the order of 4-months (Figure 4(c), 6(c), and 8(a)).*

P 13 L 11-19: Please add to your discussion of the regions that have low PAMF values a sentence that critically discusses the low model reliability in South America and particularly Europe, as most of the grid cells there have low or poor performance.

The authors agree. P13 L16-19 has been changed to:

*Examples of low-flow regions include the central United States and Australia having low PAMF regional values (Figure 8 (b)). Bi-modal regions, such as much of East Africa and Southern South America with their two rainy seasons, and constant-flow regions, such as Europe, also indicate low PAMF values (Figure 8 (b)). These flow regimes are further investigated as minor HS in section 5.*

P 13 L 26 and Figure 9: It is not clear what the Figure is showing. Is it the month with the maximum number of floods events in the DFO or the mean month of all events on record? Please specify in the text and figure caption

The authors apologize for the misunderstanding. For clarification, P13 L25-26 and the caption of Figure 9 have been changed to:

*The DFO records provide start time, end time and duration of each flooding event, as defined by the report or source, and represented as occurrence (start) month (Figure 9).*

*Figure 9. Occurrence (start) months of 3,486 events from 'Global Active Archive of Large Flood Events' from the Dartmouth Flood Observatory (DFO) over 1985-2008 (Brakenridge, 2011);*

*polygons indicate the estimated spatial extent, colors represent the start month, with most recent events in time layered on top.*

Section 5:

No suggestions; Well analysed and discussed.

Section 6

Discussion in section 4 and 6 have improved considerably.

I congratulate the authors on these sections.

No further comments.

Figures:

Fig 4 and 6: For the ease of the reading/interpreting the results, please indicate in the text or the caption of these figures that negative values mean that the simulated high flow season is earlier and that positive values mean that the simulated HS is later.

Thank you for the helpful comment. The captions for (c) Temporal difference of both Figure 4 and 6 for have been changed to:

*(c) Temporal difference in PM between observations and simulation (simulation-observation, in number of months; negative (positive) value indicates that the simulated PM is earlier (later) than the observed PM).*

Fig 5 and Fig 11: For the ease of the reading/interpreting the results, please indicate in the text that refers to these figures or in the captions what the percentages of PMAF mean. I.e. 0-40% = poor, 40-60% low, as it is already done in Figure 8.

The captions of Figure 5 and 11 have been changed to:

*Figure 5. Calculated Percentage of Annual Maximum Flow (PAMF) values for (a) 691 GRDC observation stations, and (b) simulated streamflow at associated locations; subjectively classified as high = 80-100%, moderate = 60-80%, low = 40-60%, and poor = 0-40%.*

*Figure 11. (a) Minor Peak Month (PM) for flooding as defined at detected grid cells and (b) joint PAMFs of major and minor PMs at corresponding cells; subjectively classified as high = 80-100%, moderate = 60-80%, and low = 40-60%.*

Fig9. See comment above for P 13 L 26

As indicated above, this has now been clarified.

Typography:

Please make sure that you replace the full stop inside the parenthesis with the full stop outside of the parenthesis (i.e. use ') .' instead of '.)')

Thank you for the suggestion. This has been updated accordingly.

1 **Defining High-flow Seasons using Temporal Streamflow**

2 **Patterns from a Global Model**

3 **Donghoon Lee<sup>1</sup>, Philip Ward<sup>2</sup> and Paul Block<sup>1</sup>**

4 [1]{University of Wisconsin - Madison, Madison, Wisconsin, USA}

5 [2]{Institute for Environmental Studies (IVM), VU University Amsterdam, the Netherlands}

6 Corresponding Author: Paul Block (paul.block@wisc.edu)



## 1 **Abstract**

2 Globally, flood catastrophes lead all natural hazards in terms of impacts on society, causing  
3 billions of dollars of damages annually. Here, a novel approach to defining high-flow seasons  
4 (3-month) globally is presented by identifying temporal patterns of streamflow. The main high-  
5 flow season is identified using a volume-based threshold technique and the PCR-GLOBWB  
6 model. In comparison with observations, 40% (50%) of locations at a station (sub-basin) scale  
7 have identical peak months and 81% (89%) are within 1 month, indicating fair agreement  
8 between modeled and observed high-flow seasons. Minor high-flow seasons are also defined  
9 for bi-modal flow regimes. Identified major and minor high-flow seasons together are found to  
10 well represent actual flood records from the Dartmouth Flood Observatory, further  
11 substantiating the model's ability to reproduce the appropriate high-flow season. These high  
12 spatial-resolution high-flow seasons and associated performance metrics allow for an improve  
13 understanding of temporal characterization of streamflow and flood potential, causation, and  
14 management. This is especially attractive for regions with limited observations and/or little  
15 capacity to develop early warning flood systems.

## 1 Introduction

Flood disasters rank as one of the most destructive natural hazards in terms of economic damage, causing billions of dollars of damage each year (~~Munich Re, 2012.~~)(Munich Re, 2012). These flood damages have risen starkly over the past half-century given the rapid increase in global exposure (~~Bouwer, 2011; UNISDR, 2011; Visser et al., 2014.~~)(Bouwer, 2011; UNISDR, 2011; Visser et al., 2014). To specifically address flood disasters from a global perspective, understanding of global-scale flood processes and streamflow variability is important (~~Dettinger and Diaz, 2000; Ward et al., 2014.~~)(Dettinger and Diaz, 2000; Ward et al., 2014). In recent decades, studies have investigated global-scale streamflow characteristics using observed streamflow from around the world (~~Beck et al., 2013; McMahon, 1992; McMahon et al., 2007; Peel et al., 2001, 2004; Poff et al., 2006; Probst and Tardy, 1987.~~)(Beck et al., 2013; McMahon, 1992; McMahon et al., 2007; Peel et al., 2001, 2004; Poff et al., 2006; Probst and Tardy, 1987) and modeled streamflow from global hydrological models (~~Beck et al., 2015; van Dijk et al., 2013; McCabe and Wolock, 2008; Milly et al., 2005; Ward et al., 2013, 2014.~~)(Beck et al., 2015; van Dijk et al., 2013; McCabe and Wolock, 2008; Milly et al., 2005; Ward et al., 2013, 2014) to investigate ungauged and poorly gauged basins (~~Fekete and Vörösmarty, 2007.~~)(Fekete and Vörösmarty, 2007). Despite this broad attention on annual streamflow and its connections to global climate processes and precursors, there has been relatively little attention paid to the intra-annual timing of streamflow, emphasizing the need for analysis of seasonal streamflow patterns to further improve understanding of large-scale hydrology and atmospheric behaviors on the main (flood) streamflow season globally (~~Dettinger and Diaz, 2000.~~)(Dettinger and Diaz, 2000). Moreover, better assessment of streamflow timing and seasonality is important for addressing frequency and trend analyses, flood protection and preparedness, climate-related changes, and other hydrological applications that possess important sub-annual characteristics (~~Burn and Arnell, 1993; Burn and Hag Elnur, 2002; Cunderlik and Ouarda, 2009; Hodgkins et al., 2003.~~)(Burn and Arnell, 1993; Burn and Hag Elnur, 2002; Cunderlik and Ouarda, 2009; Hodgkins et al., 2003). This motivates further investigation of intra-annual temporal streamflow patterns globally.

Only a small number of studies have investigated global-scale seasonality and temporal patterns of streamflow, with minimal focus on objective streamflow timing. ~~Haines et al. (1988)~~Haines et al. (1988) cluster 969 world rivers into 15 categories based on seasonality and average monthly streamflow data, and present one of the first maps providing a global classification. ~~Burn and Arnell (1993)~~Burn and Arnell (1993) aggregate 200 streamflow stations into 44 similar climatic regions and

1 subsequently combine these into 13 groups using hierarchical clustering based on similarity of  
2 the annual maximum flow index, providing spatial and temporal coincidences of flood response.  
3 [Dettinger and Diaz \(2000\)](#) aggregate 1345 sites into 10 clusters based on seasonality using  
4 climatological fractional monthly flows (CFMFs) to identify peak months and linkages with  
5 large-scale climate drivers.

6 In general, these studies define high streamflow or flood seasons subjectively based on the  
7 relationship between dominant streamflow amplitude patterns and large-scale climate  
8 drivers/patterns, and delineate large-scale homogeneous regions correspondingly. Defining  
9 high flow season timing is essentially a bi-product of these analyses, and may be problematic  
10 due to varying seasonal patterns (e.g. bi-modal distribution, constant or low flow areas, etc.)  
11 not captured at the large-scale delineation. There is also typically no distinguishment between  
12 minor and high flow seasons. In some cases, these minor seasons (e.g. resulting from bi-modal  
13 precipitation distribution) can produce high flow or flood conditions, and are thus of interest to  
14 identify. Here we identify high-flow seasons by capturing annual peak timing using a  
15 volumetric technique at the cell and sub-basin scale, presenting an approach focused on  
16 streamflow temporal patterns rather than pattern of amplitude. The new measure of Peak Month  
17 (PM- $\epsilon$ ) and High-flow Season (HS) coupled with the model grid scale provides much higher  
18 resolution peak timings globally than previously presented (often at large basin scale or  
19 subcontinental scale-). The performance measure introduced here (PAMF), which is Percentage  
20 of Annual Maximum Flow (PAMF), is also a new contribution relating the models ability to  
21 capture high flow season timing. These advantages are also helpful for identifying less-  
22 dominant but important seasons (minor high-flow seasons) that possess similar characteristics  
23 to the high flow season (e.g. bi-modal annual cycle), another unique contribution of this work.  
24 This leads to better temporal characterization and understanding of flood potential, causation,  
25 and management, particularly in ungauged or limited-gauged basins.

26

## 27 **2 Data description**

### 28 **2.1 Streamflow stations**

29 Daily streamflow observations utilized in this study are from the Global Runoff Data Centre  
30 ([GRDC, 2007](#)), specifically those, stations located along the global hydrology model's drainage  
31 network. Since station records that are missing even short periods may effect how a high-flow

1 season is defined, we have excluded years with any daily missing values. In this study, a  
2 minimum of 20 hydrological years is required for a station to be retained, leaving, 691 stations  
3 from all continents except Antarctica, with upstream basin areas ranging from 9,539 to  
4 4,680,000 km<sup>2</sup> and periods of record between 20 - 43 years across 1958 - 2000 (Figure 1-~~→~~).  
5 Although this criteria is admittedly quite strict (no missing 20-year daily data), including  
6 stations with missing records does not add a significant number. These stations are mostly  
7 located on large-rivers; annual streamflow of 75% of stations is larger than 100 m<sup>3</sup>/sec, 35%  
8 of stations are larger than 500 m<sup>3</sup>/sec, 20% of stations are larger than 1,000 m<sup>3</sup>/sec and 5%  
9 of stations are larger than 5,000 m<sup>3</sup>/sec.

## 10 2.2 PCR-GLOBWB

11 In this study, we evaluate simulations of daily streamflow over the period 1958-2000 taken  
12 from Ward et al. (2013), carried out using PCR-GLOBWB (PCRaster GLOBal Water Balance),  
13 a global hydrological model with a 0.5° x 0.5° resolution (~~Van Beek and Bierkens, 2009; Van~~  
14 ~~Beek et al., 2011~~)(Van Beek and Bierkens, 2009; Van Beek et al., 2011). Although the PCR-  
15 GLOBWB model is not calibrated, and simulations may contain biases and uncertainty at course  
16 spatial resolution, the long time-series of streamflow provided globally has been deemed  
17 sufficient to estimate long-term flow characteristics with spatial consistency (~~Winsemius et al.,~~  
18 ~~2013~~)(Winsemius et al., 2013). Additionally, this model has been validated in previous studies  
19 in terms of streamflow (Van Beek et al., 2011), and terrestrial water storage (Wada et al., 2011)  
20 and at stations along major rivers in the world. The model's extreme discharges are also  
21 evaluated by (Ward et al., 2013), with strong model performance. Ward et al. (2013) with fair  
22 to good performance at stations with large drainage area (≥125,000 km<sup>2</sup>), corresponding to  
23 24% of GRDC stations used in this study, excepting overestimation in several arid regions. Note  
24 that for the simulations used in this study, the maximum storage within the river channel is  
25 based on geomorphological laws that do not account for existing flood protection measures such  
26 as dikes and levees.

27 For the simulations used in this study, the PCR-GLOBWB model was forced with daily  
28 meteorological data from the WATCH (Water and Global Change) project (Weedon et al.,  
29 2011), namely precipitation, temperature, and global radiation data. These data are available at  
30 the same resolution as the hydrological model (0.5° x 0.5°-~~°~~). The WATCH forcing data were  
31 originally derived from the ERA-40 reanalysis product (~~Uppala et al., 2005~~)(Uppala et al.,

1 [2005](#)), and were subjected to a number of corrections including elevation, precipitation gauges,  
2 time-scale adjustments of daily values to reflect monthly observations, and varying atmospheric  
3 aerosol-loading. It is possible that this may have some minor effect on streamflow simulation,  
4 likely providing more realistic outcomes. Full details of corrections are described in [Weedon  
5 et al. \(2011\)](#).

### 7 **3 Defining high-flow seasons**

8 To identify spatial and temporal patterns of dominant streamflow uniformly, we design a fixed  
9 time window for representing high-flow seasons globally. Here we define major high-flow  
10 seasons as the 3-month period most likely to contain dominant streamflow and the annual  
11 maximum flow. The central month is referred to as the Peak Month (PM) and the full 3-month  
12 period is referred to as the High-flow Season (HS-~~→~~). Specifically, we define PM first, and then  
13 define HS as the period also containing the month before and after the PM. This approach is  
14 performed for both observed (station) and simulated (model) streamflow to gauge performance.

#### 15 **3.1 Methodology for defining grid-cell scale high-flow seasons**

16 In the last few decades, a number of studies have investigated the timing of peak flows in the  
17 context of analyzing flood seasonality, frequency and trends. Generally, two main properties  
18 are emphasized regarding flood timing: peak volume and peak timing. Considering peak  
19 volume, the occurrence dates are commonly recorded for a fixed-time period or specific amount  
20 of peak volume, often in the context of trend analysis. For examples, ~~Hodgkins and Dudley~~  
21 [\(2006\)Hodgkins and Dudley \(2006\)](#) use winter-spring center of volume (WSCV) dates to  
22 analyze trends in snowmelt-induced floods, and [Burn \(2008\)](#) uses percentiles of annual  
23 streamflow volume dates as indicators of flood timing, also for trend analysis. For peak timing,  
24 two sampling methods are frequently applied in hydrology. The first and most common is the  
25 annual-maximum (AM) method, which samples the largest streamflow in each year. The second  
26 method is the peaks-over-threshold (POT) method ([Smith, 1984, 1987; Todorovic and  
27 Zelenhasic, 1970](#)), in which all distinct, independent dominant peak flows greater than a fixed  
28 threshold are counted, ~~prior to a specified date.~~ In contrast to the AM method, POT can capture  
29 multiple large independent floods within a single year, including the annual maximum flow,  
30 but may ~~also missnot capture~~ the annual maximum flow in years in which streamflow is less  
31 than the pre-defined threshold; this threshold can either be defined based on a specific average

1 number of floods or a specific mean exceedance level over the entire period (Cunderlik et al.,  
2 2004a.)(Cunderlik et al., 2004a; Institute of Hydrology, 1999; Lang et al., 1999). The PM  
3 selected, therefore, is dependent on the peak properties (volume, timing) considered. For a local  
4 study, selecting the PM can be based on well-defined climatic or hydrologic characteristics (e.g.  
5 rainy season, snow-melt, etc.), however no single global method can be uniformly applied to  
6 define the PM everywhere. Thus, to define the HS, and specifically the PM, globally, both peak  
7 volume and peak timing aspects need to be considered (~~Javelle et al. 2003.)~~Javelle et al. 2003).  
8 To do this, we adopt a Volume-Based Threshold (VBT) technique. This technique is similar to  
9 a streamflow volume-based technique in terms of capturing the days (Julian dates) when  
10 streamflow exceeds the pre-defined threshold (percentile of flows) and associated volume  
11 ~~(Burn, 2008.)~~(Burn, 2008). The major difference, however, is that the VBT applies the  
12 threshold over the entire time-series (available record) concurrently instead of on a year-by-  
13 year basis. In other words, for the 95<sup>th</sup> percentile, instead of annually calculating the 95<sup>th</sup>  
14 percentile, it is calculated using the entire period of record. The common volume-based  
15 technique thus records events every year surpassing the threshold, however for the VBT  
16 approach, every year need not have a peak above the threshold. This approach emphasizes  
17 capturing the key peaks across the entire available time-series (as in a peak over threshold  
18 approach.) ~~VBT thus contains both volume and timing characteristics for defining the Peak~~  
19 ~~Month (PM.) Here we select streamflow surpassing the top 5% of flows across all years (1958-~~  
20 ~~2000) as the threshold for considering a high streamflow level; this level is commonly adopted~~  
21 ~~in threshold approaches (Burn, 2008; Mishra et al., 2011.) The month containing the greatest~~  
22 ~~number of occurrences in the top 5% is defined as the PM, and subsequently the HS is defined).~~  
23 VBT thus contains both volume and timing characteristics for defining the Peak Month (PM).  
24 Here, the month containing the greatest number of occurrences over the specified percentage of  
25 flows across all years (1958-2000) is defined as the PM, and subsequently the HS is designated  
26 as the period containing the PM plus the month before and after the PM. Figure 2 provides an  
27 example based on seven years of synthetic streamflow with the volumetric threshold set at the  
28 top 5% of flows; the number of days surpassing the 5% threshold is listed for each month. In  
29 this example, August has the largest number of days over the threshold (105 days), thus August  
30 is defined as PM and July-September is defined as HS.

31 To evaluate the defined HS objectively, by evaluating the number of annual maximum flows  
32 captured, we develop a simple evaluating statistic called the Percentage of Annual Maximum  
33 Flow (PAMF). PAMF is computed as shown in Eq. 1:

$$1 \quad PAMF(i) = \frac{\sum_{j=i-1}^{i+1} nAMF(j)}{\sum_{k=1}^{12} nAMF(k)}, \quad 1 \leq i \leq 12 \quad (1)$$

2 where  $nAMF(i)$  denotes the number of annual maximum flows that occur in month  $i$  across the  
 3 full record. In Eq. (1), when  $i$  is 1 (Jan),  $i - 1$  in the summation is 12 (Dec), and when  $i$  is 12  
 4 (Dec),  $i + 1$  is 1 (Jan). Here the PAMF provides the percentpercentage of ~~time the~~ annual  
 5 maximum flows ~~occurs~~occurring in the defined HS across the evaluation period. The PAMF is  
 6 relatively simple, yet provides clear indication of how well PM selected represents the  
 7 occurrence of annual peaks across the time-series. For example, a high PAMF indicates that the  
 8 HS is highly likely to contain the annual maximum flood each year. In contrast, a low PAMF  
 9 indicates that the timing of the annual maximum flow is more likely to vary temporally, and  
 10 may be a result of bimodal seasonality, consistently high or low streamflow throughout the year,  
 11 streamflow regulated by infrastructure or natural variation. In this study, we subjectively  
 12 classify HS PAMF values as: high = 80-100%, moderate = 60-80%, low = 40-60% and poor =  
 13 0-40%. The PAMF is calculated for both the observed streamflow at the selected 691 GRDC  
 14 stations and the simulated streamflow at the associated 691 grid locations.

15 The VBT technique is compared with the common volume-based technique and POT technique  
 16 to gauge performance. Four volume-based durations, namely V01%, V03%, V05% and V10%  
 17 and three POT techniques averaging 1, 2, and 3 peaks per year (POT1, POT2 and POT3,  
 18 respectively) are selected. For the V01% technique, the HS is simply centered on the PM  
 19 containing the largest number of occurrences of the top 1% of annual streamflow volume across  
 20 the total years available. The V03%, V05% and V10% techniques are similar to the V01%  
 21 approach, respectively using 3%, 5% and 10% of annual streamflow volume. Comparatively,  
 22 techniques with a shorter time component (1-3% of annual volume) favor identifying the PM  
 23 by peak timing, since the top 1-4 days of streamflow tend to be located near the peak, while  
 24 techniques with longer time components (5-10% of annual volume) favor identifying the PM  
 25 based on duration and peak volume, since the top 19-33 days of streamflow tend to be located  
 26 near the volumetric centroid of the hydrograph, rather than the peak, if they differ. The VBT  
 27 technique is an attempt to bridge these two criteria. For the POT techniques, independence  
 28 criteria is applied to avoid counting multiple peaks from the same event (~~Institute of Hydrology,~~  
 29 ~~1999.)(Institute of Hydrology, 1999)~~. For example, two peaks must be separated by at least  
 30 three-times the average rising time to peak, and minimum flow between two peaks must be less  
 31 than two-thirds of the higher one of the two peaks. More details of independence criteria are  
 32 described in ~~Lang et al. (1999.)~~Lang et al. (1999).

1 An analysis examining sensitivity of selected threshold levels for the VBT technique is also  
2 undertaken. Performance of thresholds representing 1%, 3%, 5% and 10% exceedance across  
3 the entire period of record, named VBT1%, VBT3%, VBT5% and VBT10%, respectively, are  
4 compared.

5 To compare techniques and thresholds, the PMs are defined at the 691 selected stations and  
6 associated model grids. The locations where the PMs differ (by at least one technique) are of  
7 most interest. This occurs at 61% of stations and 54% of associated grids. Cross-correlations  
8 of PM between the four common volume-based techniques clearly indicate the tendency of the  
9 defined PM to shift from peak timing dominated to peak volume dominated as the time  
10 component increases (Table 1-→). Correlation between VBT techniques and volume-based  
11 techniques are quite similar and consistent (0.82-0.86 and 0.84-0.86 for observed and simulated  
12 streamflow, using VBT5%; Table 1), preliminarily indicating some success in capturing both  
13 timing and volume properties, while correlation between the VBT techniques and POT are less  
14 strong (0.78-0.81 and 0.79-0.83 for observed and simulated streamflow, respectively, using  
15 VBT5%; Table 1-→). The PAMF is also useful for comparing techniques, such that the technique  
16 having the highest average PAMF typically contains more annual maximum flow events in their  
17 defined HSs. The VBT5% is superior to other VBT and POT techniques for both observed and  
18 modeled streamflow, having the highest PAMF values, however the volume-based techniques  
19 indicate similar or even slightly better performance than VBT5% (Table 2-→). This is not  
20 unexpected as the volume-based techniques are designed to capture annual peak flows on a  
21 year-by-year basis, whereas the POT and VBT recordsrecord significant peaks across the full  
22 time-series, and may “miss”not capture annual peaks in some years in which that peak is small  
23 relative to all peaks throughout the available record. -Thus VBT tends to select PMs that contain  
24 the most significant peaks overall, and subsequently have the highest potential for capturing  
25 probable flood seasons for flood-prone basins, a desirable outcome for this study. To illustrate  
26 this in the context of the PAMF, if all years are ranked for each location based on the annual  
27 peak flow, and the top 50% (half) are retained, the PAMF actually favors the VBT approach,  
28 surpassing the volume-based approach by 5-6% for PMs and 2-3% for HSs.

29 Finally, techniques may be evaluated by comparing the temporal difference (number of months)  
30 between model-based and observed PMs; closer is clearly superior. The VBT3% and VBT5%  
31 techniques produce the greatest degree of similarity between model-based and observed PMs  
32 (81% of stations having  $\pm 1$  month difference; Table 3-→). Overall, the VBT technique



1 demonstrates superior performance as compared with the POT techniques by all comparisons.  
2 The VBT technique is also on par or slightly superior to the common volume-based technique,  
3 especially considering the 5% threshold; thus, the remainder of the analysis is carried out  
4 utilizing the VBT5% technique only.

### 5 **3.2 Methodology for defining sub-basin scale high-flow seasons**

6 In addition to evaluating the HS at the 691 grid cells based on model outputs, the PM and HS  
7 can also be defined at the sub-basin scale globally where observations are present. Previous  
8 studies have investigated flood seasonality as it relates to basin characteristics; for example,  
9 basins are delineated/regionalized and grouped according to similarity/dissimilarity of  
10 streamflow seasonality (Burn, 1997; Cunderlik et al., 2004a), or conversely, flood seasonality  
11 is occasionally used to assess hydrological homogeneity of a group of regions (Cunderlik and  
12 Burn, 2002; Cunderlik et al., 2004b), thus evaluating at the sub-basin scale is warranted.

13 While defining a single PM for a large-scale basin may be convenient, it may be difficult to  
14 justify given the potentially long travel times and varying climate, topography, vegetation, etc.  
15 Additionally, infrastructure may be present to regulate flow for flood control, water supply,  
16 irrigation, recreation, navigation, and hydropower (WCD, 2000), causing managed and natural  
17 flow regimes to differ drastically. This becomes important, as globally more than 33,000 records  
18 of large dams and reservoirs are listed (ICOLD, 1998-2009), with geo-referencing available for  
19 6,862 of them (Lehner et al., 2011). Nearly 50% of large rivers with average streamflow in  
20 excess of 1,000 m<sup>3</sup>/s are significantly modulated by dams (Lehner et al., 2011), often  
21 significantly attenuating flow hydrographs and flood volumes (twenty percent of GRDC  
22 stations fall into this category→). The PAMF, as previously defined, can aid in identifying  
23 stations affected by upstream reservoirs through low PAMF values. This is applied with the  
24 assumption that reservoir flood control disperses the annual maximum flows across months  
25 rather concentrated within a few months (e.g. akin to natural flow→). In this study, we used the  
26 global sub-basins from the 30' global drainage direction map (DDM30) dataset (Döll and  
27 Lehner, 2002) with separation of large basins (Ward et al., 2014).

28 To define a sub-basin's PM, the maximum PAMF and associated PM for each station within  
29 the sub-basin are considered according to the following:

- 30 • If multiple stations exist within the sub-basin, the PM is defined as the PM occurring  
31 for the largest number of stations

- 1 • If there is a tie between months, their average PAMF values are compared, and the  
2 month having the higher average PAMF is defined as the PM.
- 3 • If there is a tie between months and equivalent average PAMF values, the month having  
4 the higher average annual streamflow is defined as the PM.

5 The sub-basin's PM is defined based on the occurrence of station or grid-level PMs rather than  
6 the PAMF values to diminish results being skewed by biased simulations or varying climate  
7 effects in small parts of the sub-basin. When there are an equal number of occurrences for  
8 different PMs, the average PAMF values are used to determine which PM is selected. In this  
9 case, the effect of stations downstream of reservoirs will be minimized given their typically low  
10 average PAMF values. assuming operational rules relatively evenly distribute the annual flow  
11 across all months; however, if operational rules instead concentrate releases to a few months,  
12 PAMF values may actually be high. This procedure is applied for both stations (observations)  
13 and corresponding grid cells (model) in each sub-basin. To illustrate, consider the 6 GRDC  
14 stations in the Zambezi River Basin (Figure 3-~~7~~). For most of the stations, the observed PM is  
15 defined as a month later than the model-based PM (Table 4), an apparent bias in the model. The  
16 PAMF of STA06 observations is noticeably lower than for other stations (36%; Table 4) given  
17 its location downstream of the Itzhi-Tezhi dam (STA05) (Figure 3-~~7~~). Otherwise, PAMF values  
18 are consistently high across all stations. March is the PM identified most often, thus the final  
19 sub-basin PM selected is March.

20 In contrast, the model-based simulated streamflow produces a high PAMF at STA06 (97%), as  
21 the Itzhi-Tezhi dam is not represented in the simulations used for this study, and subsequently  
22 does not account for modulated streamflow. Across other stations, the PAMF is also high,  
23 however an equal number of stations select February and March. In this case, February is  
24 selected as the final basin PM given its higher average PAMF value (96% vs. 91%~~-9~~%).

25 By this approach, all 691 GRDC stations are grouped into 223 sub-basins to define the PM  
26 (Figure 6-~~7~~); 58% of sub-basins are defined by a single station, only 7.6% (observations) and  
27 8.1% (model) of sub-basins have ties when defining PMs, and only one sub-basin has a tie  
28 between PMs and average PAMF values.

29

## 4 Verification of selected high-flow seasons

Model-based PMs are verified by comparing with observation-based PMs at station and sub-basin scales. Additionally, historic flood records from the Dartmouth Flood Observatory (DFO) are used to compare basin-level PMs to actual flooded areas spatially and temporally. Specifically, we apply the following information from DFO: start time, end time, duration and geographically estimated area at 3,486 flood records across 1985-2008.

### 4.1 Observed versus modeled high-flow seasons

Ideally the model-based and observed GRDC stations have fully or partially overlapping HS periods. If so, this builds confidence in interpreting HSs at locations where no observed data are available. For comparing modeled PMs to observations, the defined PMs and calculated PAMF are represented globally at the station scale (Figure 4-5) and sub-basin scale (Figure 6) with temporal differences of PMs (modeled PM – observed PM). In the southeastern United States, GRDC stations express relatively lower PAMF values for observations (40-60%) than model outputs (60-80%), due to the high level of managed infrastructure. In the central-southern United States and Europe, low PAMF values are computed for both observations and modeled output (Figure 5) with notable temporal differences (Figure 4 (c)). For observations, this is attributable, at least in part, to reservoirs and dams along the Mississippi, Missouri and Danube rivers. Additionally, relatively constant streamflow patterns are identified in both observations and modeled output, consistent with previous studies reporting these flow regimes as uniform or perpetually wet (Burn and Arnell, 1993; Dettinger and Diaz, 2000; Haines et al., 1988.) (Burn and Arnell, 1993; Dettinger and Diaz, 2000; Haines et al., 1988). Minor high-flow seasons may also play a role. Model biases also effect PM selection; for Northwestern North America, PMs for many points are defined on average one month earlier than with observations, producing moderate PAMF values (60% and higher). In Northern Europe, especially around South Finland, this becomes much more pronounced, with large differences between PMs from observations and the model, on the order of 4-months (Figure 4(c), 6(c), and 8(a)). In western and northern Australia, PMs are modeled 1-month later on average than observations excepting with two occurrences in the west (5-month difference) due to both observed and modeled low-flow conditions. Such low-flow regimes are also apparent in southeastern Australia, causing large differences between PMs (4-5 months). The differences in PMs between observations and modeled outputs are also compared at the continental scale (Figure 7). In North America, 38% of stations and 51% of sub-basins produce identical PMs, growing to 82% of stations and

1 93% of sub-basins when considering a  $\pm 1$  month temporal difference (e.g. HS; Figure 7-)). In  
2 Asia 65% of stations and 70% of sub-basins have identical PMs, growing to 90% of stations  
3 and 92% of sub-basins with  $\pm 1$  month temporal difference (Figure 7-)). In central Russia, a large  
4 difference between PMs ( $\pm 3$  months) are attributable to reservoirs on the Yenisei and Angara  
5 rivers and model bias (Figure 4 (c)). In Africa, 48% of stations and 60% of sub-basins produce  
6 identical PMs (Figure 7), 30% of stations and 27% of sub-basins are modeled 1-month earlier,  
7 and 7.4% of stations and 6.7% of sub-basins are modeled 1-month later than observation (Figure  
8 7-)). In South America, with only 5 stations, 40% have the same month, 40% are modeled 1-  
9 month earlier and 20% of stations are modeled 2-months earlier than observations.

10 Comparing observations and modeled output globally, 40% of the locations share the same PM.  
11 The model's bias is one of main reasons for this moderate performance; other important  
12 contributors include minor high-flow seasons, perpetually wet or dry regions, and  
13 anthropogenic effects such as reservoir regulation. Considering a difference of  $\pm 1$  month, this  
14 jumps to 81%, and 91% for  $\pm 2$  months (Figure 7-)). From a sub-basin perspective, the  
15 similarities are even stronger (50% identical PM, 88%  $\pm 1$  month and 92%  $\pm 2$  month),  
16 indicating a relatively high level of agreement. For locations having dissimilar PMs ( $\geq \pm 3$   
17 months, 9% of locations and 8% of sub-basins), a substantial portion are located downstream  
18 of reservoirs directly, such as STA06 in the Zambezi example (Table 4), or are low-flow (dry)  
19 or constant-flow locations, both producing exceedingly low PAMF values. Differences in PMs  
20 are not unexpected for low-flow and constant-flow locations, given the propensity for the annual  
21 streamflow maximum to potentially occur in a wide number of months. Overall, however, as  
22 more than 80% of both stations and sub-basins have similar PMs ( $\pm 1$  month), it appears that  
23 the global water balance model performs appropriately well in defining high-flow seasons  
24 globally at locations where observations are available.

25 This may be subsequently extended to defining PMs and PAMF at all grid cells (Figure 8-)).  
26 Generally, low and poor PAMF values (0-60%) indicate a naturally unstable annual maximum  
27 flow (no clear high-flow season), which occurs in cases of constant-flow, low-flow, bi-modal  
28 flow and regulated flow. All cases, except regulated flow, are simulated within the PCR-  
29 GLOBWB simulations used, thus the cell-based PAMF values (Figure 8 (b)) can provide a  
30 sense of confidence for the defined PM (Figure 8 (a-))). Examples of low-flow regions include  
31 the central United States and Australia having low PAMF regional values (Figure 8 (b-))). Bi-  
32 modal regions, such as much of East Africa and Southern South America with ~~its~~their two rainy  
33 seasons, may and constant-flow regions, such as Europe, also ~~be associated with~~indicate low

1 PAMF values. ~~(Figure 8 (b). These flow regimes are further investigated as minor HS in section~~  
2 ~~5.~~

## 3 **4.2 Modeled high-flow seasons versus actual flood records**

4 Model-based PMs may also be verified (subjectively) by surveying historic flood records. One  
5 such source is the Dartmouth Flood Observatory (DFO), a large, publically accessible  
6 repository of major flood events globally over 1985-2008, based on media and governmental  
7 reports and instrumental and remote sensing sources. Delineations of affected areas are best  
8 estimates ~~(Brakenridge, 2011.) The DFO records provide duration of each flooding event, as~~  
9 ~~defined by the report or source, and represented as occurrence month (Figure 9.)~~~~(Brakenridge,~~  
10 ~~2011). The DFO records provide start time, end time and duration of each flooding event, as~~  
11 ~~defined by the report or source, and represented as occurrence (start) month (Figure 9).~~ DFO  
12 flood events and grid cell based PMs (Figure 8 (a)) may be compared outright, however their  
13 characteristics differ slightly. The DFO covers 1985-2008 while the model represents 1958-  
14 2000. Also, the model-based PM represents the month most likely for a flood to occur; the DFO  
15 is simply a reporting of when the event did occur, regardless of whether it fell in the expected  
16 high-flow season or not. Nevertheless, model-based PMs and historic flood records illustrate  
17 similarity (compare Figures 8 (a) and 9), particularly when both the major and minor high flow  
18 seasons are considered, further indicating merit in the ability of the proposed approach to  
19 identify the PM. Consistently, regions with high model-based PAMF (80-100%), such as  
20 Eastern South America, Central Africa and Central Asia, tend to agree well with DFO records,  
21 while poor or less than poor PAMF (0-60%) regions, such as Central North America, Europe,  
22 and East Africa, tend not to be in agreement with DFO records. In these low PAMF regions,  
23 however, DFO records also illustrate floods occurring sporadically throughout the year, further  
24 supporting accordance between cell-based PAMF and DFO records (Figures 8 (b) and 9-)).

## 26 **5 Defining minor high-flow seasons**

27 In some climatic regions, there is no one single, well-defined flood season. For example, East  
28 Africa has two rainy seasons, the major season from June to September and the minor season  
29 from January to April/May. These two seasons are induced by northward and southward shifts  
30 of the inter-tropical convergence zone (ITCZ) ~~(Seleshi and Zanke, 2004.)~~~~(Seleshi and Zanke,~~  
31 ~~2004).~~ This bi-modal East African pattern allows for potential flooding in either season. In

1 Canada, as another example, the dominant spring snowmelt season (Mar-May) and fall rainy  
2 season (Aug-Oct) allow for flood occurrences in either period (~~Cunderlik and Ouarda,~~  
3 ~~2009~~)(Cunderlik and Ouarda, 2009).

4 Previous studies have investigated techniques to differentiate seasonality from uni-, bi- and  
5 multi-modal streamflow climatologies and evaluate trends in timing and magnitude of  
6 streamflow, including the POT method, directional statistics method, and relative flood  
7 frequency method (Cunderlik and Ouarda, 2009; Cunderlik et al., 2004a). These methods may  
8 perform well at the local (case-specific) scale to define minor high-flow seasons, however  
9 applying them uniformly at the global scale can be problematic, given spatial heterogeneity.  
10 Additionally, even though bimodal streamflow climatology may be detected, the magnitude of  
11 streamflow in the minor season may or may not be negligible in regards to flooding potential  
12 as compared with the major season.

13 To detect noteworthy minor high-flow seasons globally, we classify streamflow regimes by  
14 climatology and monthly PAMF value, calculated using Eq. (1) at each month (Figure 10-~~→~~).  
15 Classifications include unimodal, bimodal, constant, and low-flow. The unimodal streamflow  
16 climatology has high values of PAMF around the PM; the bi-modal classification is represented  
17 by two peaks of PAMF (and may therefore contain a minor season); both constant and low-  
18 flow classifications represent low values of PAMF between months. Distinguishing between  
19 bi-modal and other classifications is nontrivial. For example, initial inspection of the constant  
20 streamflow classification (both climatology and monthly PAMF, Figure 10 (c)) could be  
21 mistaken for a non-dominant bi-modal distribution. We adopt the following criteria to  
22 differentiate bi-modal streamflow from uni-modal, constant, and low-flow conditions.

- 23 • The low-flow classification is defined for annual average streamflow less than  $1 \text{ m}^3/\text{sec}$ .
- 24 • The major and minor PMs must be separated by at least two months in order to prevent  
25 an overlap of each HS (3-month-~~→~~).
- 26 • If there is a peak in the monthly PAMF values outside the major HS, it is regarded as a  
27 *potential* minor PM. If the sum of the major and *potential* minor PM's PAMF is greater  
28 than 60% (minimum of 29 out of 43 annual maximums fall in one of the HS), the  
29 *potential* minor PM is confirmed as a minor PM; the major PM's PAMF cannot exceed  
30 80%.

31 A *potential* minor PM is identified by a secondary peak in the monthly PAMF rather than the  
32 magnitude or shape of streamflow. A minor HS is not defined when a major PM's PAMF is

1 greater than 80% (minimum of 35 out of 43 annual maximums), indicating a robust uni-modal  
2 streamflow character (Figure 10 (a)). The sum of both major and minor PM's PAMF (joint  
3 PAMF) is used to determine the likelihood that one of the HSs contains the annual maximum  
4 flow; a high value of the joint PAMFs (80-100%) indicates strong likelihood (Figure 10 (b)),  
5 moderate values (60-80%) imply moderate likelihood, with some probability of being classified  
6 as constant streamflow (Figure 10 (c)); low values (40-60%) are likely constant or low  
7 streamflow (Figure 10 (d)). Minor HSs are similar to major HSs, containing the minor PM and  
8 the month before and after. Minor HSs are evident in the tropics and sub-tropics and are  
9 spatially consistent with bi-modal rainfall regimes discovered by [Wang \(1994\)](#) (Figure 11-~~→~~).  
10 Examples include East Africa (second rainy season in winter) and Canada (rainfall-dominated  
11 runoff in autumn) both having high joint PAMF values (80-100%-~~→~~%). Additional examples  
12 include the major HS (NDJ) and minor HS (MAM) in Central Africa consistent with the  
13 latitudinal movement of the ITCZ, intra-Americas' major HS (ASON) and minor HS (AMJJ)  
14 (~~Chen and Taylor, 2002~~)([Chen and Taylor, 2002](#)), and coastal regions of British Columbia in  
15 Canada and southern Alaska's minor HS (SOND) due to wintertime migration of the Aleutian  
16 low from the central north Pacific (Figure 11-~~→~~). Distinct runoff process controlled by different  
17 climate and hydrology systems can induce a bi-modal peak within a large-scale basin, such as  
18 the upstream sections of the Yenisey and Lena river systems in Russia where the major HS  
19 (AMJ) is dominated by snowmelt and the minor HS (JAS) is spurred on by the Asian monsoon.  
20 The same mechanism produces minor HSs around the extents of the Asian summer monsoon  
21 (90-100% of sum of PAMFs) (Figure 8 (b) and 11-~~→~~). Moderate minor HSs include, for  
22 example, the southern United States' (Texas and Oklahoma) bi-modal rainfall pattern (AMJ  
23 and SON) and in the southwestern United States (Arizona) where the summertime major HS  
24 (JJA) is produced by the North American monsoon and the wintertime minor HS (DJF) is  
25 affected by the regional large-scale low pressure system ([Woodhouse, 1997](#)). Southeastern  
26 Brazil's summertime major HS (NDJF) and post-summer minor HS (AMJ) are dominated by  
27 formation and migration of the South Atlantic Convergence Zone ([Herdies, 2002](#); [Lima and](#)  
28 [Satyamurty, 2010](#)). In central and eastern Europe, the major HS (FMAM) and minor HS (JJA)  
29 are defined as moderate (60-80% of joint PAMF values for central Europe and 70%-90% for  
30 eastern Europe), indicating that a minor HS is not overly pronounced; for northeastern Europe  
31 the major HS (MAM) and minor HS (NDJ) contain high joint PAMF values (80%-100%-~~→~~%).  
32 For the major HS and minor HS with joint PAMF values exceeding 60% (Figure 12), flood  
33 records (DFO) occurring over more than one month are counted in each month based on the

1 reported duration. Although one distinct flood event may dominate a monthly DFO record,  
2 strong similarity is evident between the HSs and monthly flood records (Figure 12-~~7~~). Minor  
3 HSs with high PAMF values corresponding well with observed DFO flood records include East  
4 Africa (bi-modal streamflow), the intra-Americas, and Northern Asia; only a few reported flood  
5 records occur in the minor HSs in high latitudes.

## 6 7 **6 Conclusions and Discussion**

8 In this study, a novel approach to defining high-flow seasons globally is presented by  
9 identifying temporal patterns of streamflow objectively. Simulations of daily streamflow from  
10 the PCR-GLOBWB model are evaluated to define the dominant and minor high-flow seasons  
11 globally. In order to consider both peak volume and peak timing, a volume-based threshold  
12 technique is applied to define the high-flow season and is subsequently evaluated by the PAMF.  
13 To verify model defined high-flow seasons, we compare with observations at both station and  
14 sub-basin scales. As a result, 40% of stations and 50% of sub-basins have identical peak months  
15 and 81% of stations and 89% of sub-basins are within 1 month, thus well capturing high flow  
16 seasons. When considering anthropogenic effects and bi-modal or perpetually wet/dry flow  
17 regions, these results indicate fair agreement between modeled and observed high-flow seasons.  
18 Regions expressing bi-modal streamflow climatology are also defined to illustrate potential for  
19 noteworthy secondary (minor) high-flow seasons. Model defined major and minor high-flow  
20 seasons are additionally found to represent actual flood records from the Dartmouth Flood  
21 Observatory, further substantiating the models ability to reproduce the appropriate high-flow  
22 season.

23 Large-scale temporal phenomena associated with the defined major and minor high-flow  
24 seasons are also identified. For example, global monsoon systems are clearly evident, as driven  
25 by the ITCZ, in central and eastern Africa, Asia and northern South America (Figure 8-~~7~~).  
26 Latitudinal patterns in the extra-tropics are also quite distinct, with high-flow seasons often  
27 occurring across similar months in the year. These broad temporal patterns are consistent with  
28 previous findings (~~e.g. Burn and Arnell, 1993; Dettinger and Diaz, 2000; Haines et al.,~~  
29 ~~1988~~)(e.g. Burn and Arnell, 1993; Dettinger and Diaz, 2000; Haines et al., 1988), however this  
30 analysis goes further by not being constrained to large-scale patterns for seasonal definition (via  
31 clustering) and also providing a sense of the reliability of the defined high-flow seasons.  
32 Specifically, the defined PM (Figure 8 (a)) has extended [Dettinger and Diaz \(2000\)](#)'s Peak



1 Months by focusing on basin and grid scale streamflow volumes and providing likelihood type  
2 maps using the PMAF metric developed here (e.g. Figure 8 (b)) to represent the reliability of  
3 the defined PM. This can provide a clear sense of whether the identified high-flow season is  
4 pronounced or vague. The identification of minor high-flow seasons and deciphering bi-modal  
5 from constant streamflow regimes is another notable contribution of this study; minor seasons  
6 have not been well identified in previous studies. These identified high-flow seasons are also  
7 consistent with DFO flood records both spatially and temporally, further substantiating their  
8 appropriateness.

9 Although biased simulations may theoretically contribute to a misidentified high-flow season,  
10 the global hydrological model's acceptable ability to define high-flow seasons is highlighted in  
11 this study. The global hydrological model's ability to define major and minor high-flow seasons  
12 at high resolution is highlighted in this study. Although results indicate relatively positive  
13 performance overall, regional performance varies spatially. This is advantageous for many  
14 reasons, including hydrologic assessment in ungauged and poorly gauged basins and also for  
15 investigating flood season timing within large basins having diverse physical processes, for  
16 example, how the PM may shift along long rivers (e.g. Congo River) or basins with both  
17 snowmelt and rain-dominated processes. These spatially heterogeneous high-flow seasons at  
18 high resolution have the potential to better characterize streamflow regimes than previous  
19 studies (e.g. [Dettinger and Diaz, 2000](#); [Haines et al., 1988](#)). Additional analysis to include  
20 upstream management and regulations is required to further classify global streamflow regimes  
21 and major high-flow seasons (or the elimination of them) for specific subbasin-level hydrologic  
22 applications.

23

24 *Acknowledgements.* The first author was partially funded by a grant from the University of  
25 Wisconsin-Madison. The second author was funded by a VENI grant from the Netherlands  
26 Organisation for Scientific Research (NWO).

## 1 **References**

- 2 Beck, H. E., van Dijk, A. I. J. M., Miralles, D. G., de Jeu, R. A. M., Sampurno Bruijnzeel, L.  
3 A., McVicar, T. R. and Schellekens, J.: Global patterns in base flow index and recession based  
4 on streamflow observations from 3394 catchments, *Water Resour. Res.*, 49(12), 7843–7863,  
5 doi:10.1002/2013WR013918, 2013.
- 6 Beck, H. E., de Roo, A. and van Dijk, A. I. J. M.: Global Maps of Streamflow Characteristics  
7 Based on Observations from Several Thousand Catchments\*, *J. Hydrometeorol.*, 16(4), 1478–  
8 1501, doi:10.1175/JHM-D-14-0155.1, 2015.
- 9 Van Beek, L. P. H. and Bierkens, M. F. P.: The Global Hydrological Model PCR-GLOBWB:  
10 Conceptualization, Parameterization and Verification, Utrecht., 2009.
- 11 Van Beek, L. P. H., Wada, Y. and Bierkens, M. F. P.: Global monthly water stress: 1. Water  
12 balance and water availability, *Water Resour. Res.*, 47(7), W07517,  
13 doi:10.1029/2010WR009791, 2011.
- 14 Bouwer, L. M.: Have Disaster Losses Increased Due to Anthropogenic Climate Change?, *Bull.*  
15 *Am. Meteorol. Soc.*, 92(1), 39–46, doi:10.1175/2010BAMS3092.1, 2011.
- 16 Brakenridge, G. R.: Global Active Archive of Large Flood Events, Dartmouth Flood  
17 Observatory, University of Colorado. [online] Available from:  
18 <http://floodobservatory.colorado.edu/Archives/index.html>, 2011.
- 19 Burn, D. H.: Catchment similarity for regional flood frequency analysis using seasonality  
20 measures, *J. Hydrol.*, 202(1-4), 212–230, doi:10.1016/S0022-1694(97)00068-1, 1997.
- 21 Burn, D. H.: Climatic influences on streamflow timing in the headwaters of the Mackenzie  
22 River Basin, *J. Hydrol.*, 352, 225–238, doi:10.1016/j.jhydrol.2008.01.019, 2008.
- 23 Burn, D. H. and Arnell, N. W.: Synchronicity in global flood responses, *J. Hydrol.*, 144(1-4),  
24 381–404, doi:10.1016/0022-1694(93)90181-8, 1993.
- 25 Burn, D. H. and Hag Elnur, M. a.: Detection of hydrologic trends and variability, *J. Hydrol.*,  
26 255(1-4), 107–122, doi:10.1016/S0022-1694(01)00514-5, 2002.
- 27 Chen, [aA](#). A. and Taylor, M. [aA](#).: Investigating the link between early season Caribbean rainfall  
28 and the El Nino+1 year, *Int. J. Climatol.*, 22(1), 87–106, doi:10.1002/joc.711, 2002.
- 29 Cunderlik, J. M. and Burn, D. H.: Local and Regional Trends in Monthly Maximum Flows in  
30 Southern British Columbia, *Can. Water Resour. J.*, 27(2), 191–212, doi:10.4296/cwrj2702191,  
31 2002.
- 32 Cunderlik, J. M. and Ouarda, T. B. M. J.: Trends in the timing and magnitude of floods in  
33 Canada, *J. Hydrol.*, 375(3-4), 471–480, doi:10.1016/j.jhydrol.2009.06.050, 2009.
- 34 Cunderlik, J. M., Ouarda, T. B. M. J. and Bobée, B.: Determination of flood seasonality from  
35 hydrological records / Détermination de la saisonnalité des crues à partir de séries

- 1 hydrologiques, *Hydrol. Sci. J.*, 49(3), 511–526, doi:10.1623/hysj.49.3.511.54351, 2004a.
- 2 Cunderlik, J. M., Ouarda, T. B. M. J. and Bobée, B.: On the objective identification of flood  
3 seasons, *Water Resour. Res.*, 40(1), n/a–n/a, doi:10.1029/2003WR002295, 2004b.
- 4 Dettinger, M. D. and Diaz, H. F.: Global Characteristics of Stream Flow Seasonality and  
5 Variability, *J. Hydrometeorol.*, 1(4), 289–310, doi:10.1175/1525-  
6 7541(2000)001<0289:GCOSFS>2.0.CO;2, 2000.
- 7 **Vannan** Dijk, A. I. J. M., Peña-Arancibia, J. L., Wood, E. F., Sheffield, J. and Beck, H. E.:  
8 Global analysis of seasonal streamflow predictability using an ensemble prediction system and  
9 observations from 6192 small catchments worldwide, *Water Resour. Res.*, 49(5), 2729–2746,  
10 doi:10.1002/wrcr.20251, 2013.
- 11 Döll, P. and Lehner, B.: Validation of a new global 30-min drainage direction map, *J. Hydrol.*,  
12 258(1-4), 214–231, doi:10.1016/S0022-1694(01)00565-0, 2002.
- 13 Fekete, B. M. and Vörösmarty, C. J.: The current status of global river discharge monitoring  
14 and potential new technologies complementing traditional discharge measurements, *Predict.*  
15 *Ungauged Basins PUB Kick-off (Proceedings PUB Kick-off Meet. held Bras. Novemb. 2002)*,  
16 IAHS Publ. no. 309, 129–136, 2007.
- 17 Global Runoff Data Centre: Major River Basins of the World / Global Runoff Data Centre,  
18 Koblenz, Germany: Federal Institute of Hydrology (BfG). [online] Available from:  
19 <http://grdc.bafg.de>, 2007.
- 20 Guha-Sapir, D., Hoyois, P. and Below, R.: Annual Disaster Statistical Review 2013: The  
21 Numbers and Trends, Brussels: CRED., 2014.
- 22 Haines, **aA**. T., Finlayson, B. L. and McMahon, T. **aA**.: A global classification of river regimes,  
23 *Appl. Geogr.*, 8(4), 255–272, doi:10.1016/0143-6228(88)90035-5, 1988.
- 24 Herdies, D. L.: Moisture budget of the bimodal pattern of the summer circulation over South  
25 America, *J. Geophys. Res.*, 107(D20), 8075, doi:10.1029/2001JD000997, 2002.
- 26 Hodgkins, G. A. and Dudley, R. W.: Changes in the timing of winter-spring streamflows in  
27 eastern North America, 1913-2002, *Geophys. Res. Lett.*, 33, 1–5, doi:10.1029/2005GL025593,  
28 2006.
- 29 Hodgkins, G. A., Dudley, R. W. and Huntington, T. G.: Changes in the timing of high river  
30 flows in New England over the 20th Century, *J. Hydrol.*, 278(1-4), 244–252,  
31 doi:10.1016/S0022-1694(03)00155-0, 2003.
- 32 ICOLD (International Commission on Large Dams): World Register of Dams. Version updates  
33 1998-2009, Paris: ICOLD. [online] Available from: [www.icold-cigb.net](http://www.icold-cigb.net), 2009.
- 34 Institute of Hydrology: Flood Estimation Handbook, vol. 3., Institute of Hydrology,  
35 Wallingford, UK., 1999.

- 1 Javelle, P., Ouarda, T. B. M. J. and Bobée, B.: Spring flood analysis using the flood-duration-  
2 frequency approach: application to the provinces of Quebec and Ontario, Canada, *Hydrol.*  
3 *Process.*, 17(18), 3717–3736, doi:10.1002/hyp.1349, 2003.
- 4 Lang, M., Ouarda, T. B. M. J. and Bobée, B.: Towards operational guidelines for over-threshold  
5 modeling, *J. Hydrol.*, 225(3-4), 103–117, doi:10.1016/S0022-1694(99)00167-5, 1999.
- 6 Lehner, B., Liermann, C. R., Revenga, C., Vörösmarty, C., Fekete, B., Crouzet, P., Döll, P.,  
7 Endejan, M., Frenken, K., Magome, J., Nilsson, C., Robertson, J. C., Rödel, R., Sindorf, N. and  
8 Wisser, D.: High-resolution mapping of the world's reservoirs and dams for sustainable river-  
9 flow management, *Front. Ecol. Environ.*, 9(9), 494–502, doi:10.1890/100125, 2011.
- 10 Lima, K. C. and Satyamurty, P.: Post-summer heavy rainfall events in Southeast Brazil  
11 associated with South Atlantic Convergence Zone, *Atmos. Sci. Lett.*, 11(1), n/a–n/a,  
12 doi:10.1002/asl.246, 2010.
- 13 McCabe, G. J. and Wolock, D. M.: Joint Variability of Global Runoff and Global Sea Surface  
14 Temperatures, *J. Hydrometeorol.*, 9(4), 816–824, doi:10.1175/2008JHM943.1, 2008.
- 15 McMahon, T. A.: *Global runoff: continental comparisons of annual flows and peak discharges*,  
16 Catena Verlag, Cremlingen-Destedt, Germany., 1992.
- 17 McMahon, T. [aA.](#), Vogel, R. M., Peel, M. C. and Pegram, G. G. S.: Global streamflows – Part  
18 1: Characteristics of annual streamflows, *J. Hydrol.*, 347(3-4), 243–259,  
19 doi:10.1016/j.jhydrol.2007.09.002, 2007.
- 20 Milly, P. C. D., Dunne, K. [aA.](#) and Vecchia, [aA.](#) V: Global pattern of trends in streamflow and  
21 water availability in a changing climate, *Nature*, 438(7066), 347–350,  
22 doi:10.1038/nature04312, 2005.
- 23 ~~Mishra, A. K., Singh, V. P. and Özger, M.: Seasonal streamflow extremes in Texas river  
24 basins: Uncertainty, trends, and teleconnections, *J. Geophys. Res. Atmos.*, 116(8), 1–28,  
25 doi:10.1029/2010JD014597, 2011.~~
- 26 Munich Re: Topics Geo 2012 Issue. Natural Catastrophes 2011. Analyses, Assessments,  
27 Positions, Münchener Rückversicherungs-Gesellschaft, Munich., 2012.
- 28 Peel, M. C., McMahon, T. [aA.](#) and Finlayson, B. L.: Continental differences in the variability  
29 of annual runoff-update and reassessment, *J. Hydrol.*, 295(1-4), 185–197,  
30 doi:10.1016/j.jhydrol.2004.03.004, 2004.
- 31 Peel, M. C., McMahon, T. A., Finlayson, B. L. and Watson, F. G. R.: Identification and  
32 explanation of continental differences in the variability of annual runoff, *J. Hydrol.*, 250(1-4),  
33 224–240, doi:10.1016/S0022-1694(01)00438-3, 2001.
- 34 Poff, N. L., Olden, J. D., Pepin, D. M. and Bledsoe, B. P.: Placing global stream flow variability  
35 in geographic and geomorphic contexts, *River Res. Appl.*, 22(2), 149–166, doi:10.1002/rra.902,  
36 2006.

- 1 Probst, J. L. and Tardy, Y.: Long range streamflow and world continental runoff fluctuations  
2 since the beginning of this century, *J. Hydrol.*, 94(3-4), 289–311, doi:10.1016/0022-  
3 1694(87)90057-6, 1987.
- 4 Seleshi, Y. and Zanke, U.: Recent changes in rainfall and rainy days in Ethiopia, *Int. J.*  
5 *Climatol.*, 24(8), 973–983, doi:10.1002/joc.1052, 2004.
- 6 Smith, R. L.: Threshold Methods for Sample Extremes, in *Statistical Extremes and*  
7 *Applications*, pp. 621–638, D. Reidel, Dordrech, Netherlands., 1984.
- 8 Smith, R. L.: Estimating Tails of Probability Distributions, *Ann. Stat.*, 15(3), 1174–1207,  
9 doi:10.1214/aos/1176350499, 1987.
- 10 Todorovic, P. and Zelenhasic, E.: A Stochastic Model for Flood Analysis, *Water Resour. Res.*,  
11 6(6), 1641–1648, doi:10.1029/WR006i006p01641, 1970.
- 12 UNISDR: Global Assessment Report on Disaster Risk Reduction (GAR 11) - Revealing Risk,  
13 Redefining Development, Geneva, Switzerland: United Nations Office for Disaster Risk  
14 Reduction (UNISDR)., 2011.
- 15 Uppala, S. M., KÅllberg, P. W., Simmons, [aA](#). J., Andrae, U., Bechtold, V. D. C., Fiorino, M.,  
16 Gibson, J. K., Haseler, J., Hernandez, A., Kelly, G. [aA](#)., Li, X., Onogi, K., Saarinen, S., Sokka,  
17 N., Allan, R. P., Andersson, E., Arpe, K., Balmaseda, M. [aA](#)., Beljaars, [aA](#). C. M., Berg, L. Van  
18 De, Bidlot, J., Bormann, N., Caires, S., Chevallier, F., Dethof, A., Dragosavac, M., Fisher, M.,  
19 Fuentes, M., Hagemann, S., Hólm, E., Hoskins, B. J., Isaksen, L., Janssen, P. [aA](#). E. M., Jenne,  
20 R., McNally, [aA](#). P., Mahfouf, J.-F., Morcrette, J.-J., Rayner, N. [aA](#)., Saunders, R. W., Simon,  
21 P., Sterl, A., Trenberth, K. E., Untch, A., Vasiljevic, D., Viterbo, P. and Woollen, J.: The ERA-  
22 40 re-analysis, *Q. J. R. Meteorol. Soc.*, 131(612), 2961–3012, doi:10.1256/qj.04.176, 2005.
- 23 Visser, H., Petersen, A. C. and Ligtoet, W.: On the relation between weather-related disaster  
24 impacts, vulnerability and climate change, *Clim. Change*, 461–477, doi:10.1007/s10584-014-  
25 1179-z, 2014.
- 26 Wada, Y., van Beek, L. P. H., Viviroli, D., Dürr, H. H., Weingartner, R. and Bierkens, M. F.  
27 P.: Global monthly water stress: 2. Water demand and severity of water stress, *Water Resour.*  
28 *Res.*, 47(7), n/a–n/a, doi:10.1029/2010WR009792, 2011.
- 29 Wang, B.: Climatic Regimes of Tropical Convection and Rainfall, *J. Clim.*, 7(7), 1109–1118,  
30 doi:10.1175/1520-0442(1994)007<1109:CROTCA>2.0.CO;2, 1994.
- 31 Ward, P. J., Eisner, S., Flörke, M., Dettinger, M. D. and Kummerow, M.: Annual flood sensitivities  
32 to El Niño–Southern Oscillation at the global scale, *Hydrol. Earth Syst. Sci.*, 18(1), 47–66,  
33 doi:10.5194/hess-18-47-2014, 2014.
- 34 Ward, P. J., Jongman, B., Weiland, F. S., Bouwman, A., van Beek, R., Bierkens, M. F. P.,  
35 Ligtoet, W. and Winsemius, H. C.: Assessing flood risk at the global scale: Model setup,  
36 results, and sensitivity, *Environ. Res. Lett.*, 8(4), 44019, doi:10.1088/1748-9326/8/4/044019,

- 1 2013.
- 2 WCD (World Commission on Dams): Dams and development: a framework for decision  
3 making, London, UK: Earthscan., 2000.
- 4 Weedon, G. P., Gomes, S., Viterbo, P., Shuttleworth, W. J., Blyth, E., Österle, H., Adam, J. C.,  
5 Bellouin, N., Boucher, O. and Best, M.: Creation of the WATCH Forcing Data and Its Use to  
6 Assess Global and Regional Reference Crop Evaporation over Land during the Twentieth  
7 Century, *J. Hydrometeorol.*, 12(5), 823–848, doi:10.1175/2011JHM1369.1, 2011.
- 8 Winsemius, H. C., Van Beek, L. P. H., Jongman, B., Ward, P. J. and Bouwman, ~~a~~A.: A  
9 framework for global river flood risk assessments, *Hydrol. Earth Syst. Sci.*, 17(5), 1871–1892,  
10 doi:10.5194/hess-17-1871-2013, 2013.
- 11 Woodhouse, C. A.: Winter climate and atmospheric circulation patterns in the Sonoran desert  
12 region, USA, *Int. J. Climatol.*, 17(8), 859–873, doi:10.1002/(SICI)1097-  
13 0088(19970630)17:8<859::AID-JOC158>3.0.CO;2-S, 1997.

14

- 1 Table 1. Cross-correlations of Peak Month (PM) ~~for each~~ at locations where the PMs differ by at least one classification technique ~~for~~  
 2 ~~observed and simulated streamflow where~~ (occurs at 61% of stations having different PMs and 54% of associated grids).

Classification Technique		VBT1%	VBT3%	VBT5%	VBT10%	V01%	V03%	V05%	V10%	POT1	POT2	POT3
Observed	VBT1%	1.00										
	VBT3%	0.90	1.00									
	VBT5%	0.85	0.94	1.00								
	VBT10%	0.79	0.86	0.91	1.00							
	V01%	0.82	0.82	0.82	0.81	1.00						
	V03%	0.81	0.84	0.83	0.84	0.89	1.00					
	V05%	0.81	0.85	0.86	0.85	0.86	0.92	1.00				
	V10%	0.80	0.84	0.85	0.87	0.83	0.88	0.96	1.00			
	POT1	0.78	0.78	0.78	0.74	0.76	0.77	0.76	0.74	1.00		
	POT2	0.74	0.78	0.78	0.78	0.80	0.80	0.82	0.81	0.81	1.00	
POT3	0.77	0.81	0.81	0.80	0.80	0.81	0.83	0.81	0.86	0.93	1.00	
Simulated	VBT1%	1.00										
	VBT3%	0.87	1.00									
	VBT5%	0.83	0.95	1.00								
	VBT10%	0.80	0.88	0.90	1.00							
	V01%	0.86	0.85	0.84	0.84	1.00						
	V03%	0.87	0.86	0.85	0.83	0.92	1.00					
	V05%	0.87	0.88	0.85	0.84	0.90	0.97	1.00				
	V10%	0.82	0.87	0.86	0.85	0.83	0.89	0.92	1.00			
	POT1	0.80	0.83	0.83	0.81	0.83	0.86	0.86	0.82	1.00		
	POT2	0.78	0.81	0.80	0.79	0.79	0.83	0.83	0.82	0.92	1.00	
POT3	0.80	0.81	0.79	0.80	0.80	0.83	0.84	0.81	0.92	0.95	1.00	

3

1 Table 2. Average PAMF of each classification technique for modeled and observed where stations having different PMs.

Section	VBT1%	VBT3%	VBT5%	VBT10%	V01%	V03%	V05%	V10%	POT1	POT2	POT3
Observed	60.8%	61.7%	62.0%	62.0%	63.4%	63.6%	63.0%	62.5%	60.8%	59.1%	60.6%
Simulated	63.5%	64.5%	64.7%	63.5%	65.1%	64.8%	64.9%	64.1%	63.1%	60.3%	61.9%

2



1 Table 3. Percentage of stations according to the difference in PMs between modeled and observed streamflow at each classification technique.

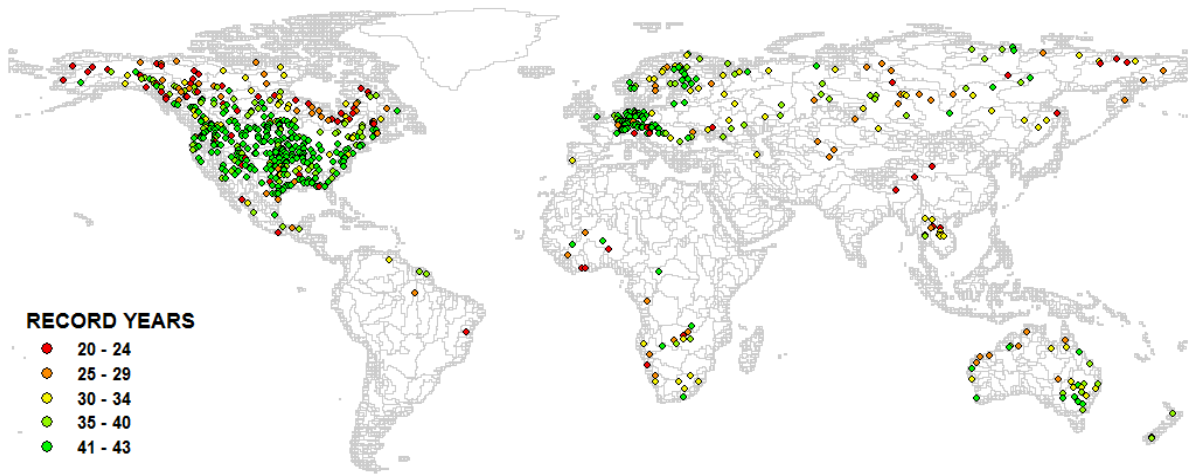
Difference in PMs	VBT1%	VBT3%	VBT5%	VBT10%	V01%	V03%	V05%	V10%	POT1	POT2	POT3
Same	39%	39%	40%	42%	38%	39%	40%	42%	38%	36%	38%
$\leq \pm 1$ month	80%	81%	81%	80%	78%	79%	79%	79%	75%	75%	77%
$\leq \pm 2$ month	90%	91%	91%	90%	89%	90%	89%	89%	87%	87%	88%
$\leq \pm 3$ month	94%	95%	95%	95%	94%	95%	95%	95%	93%	93%	94%

2

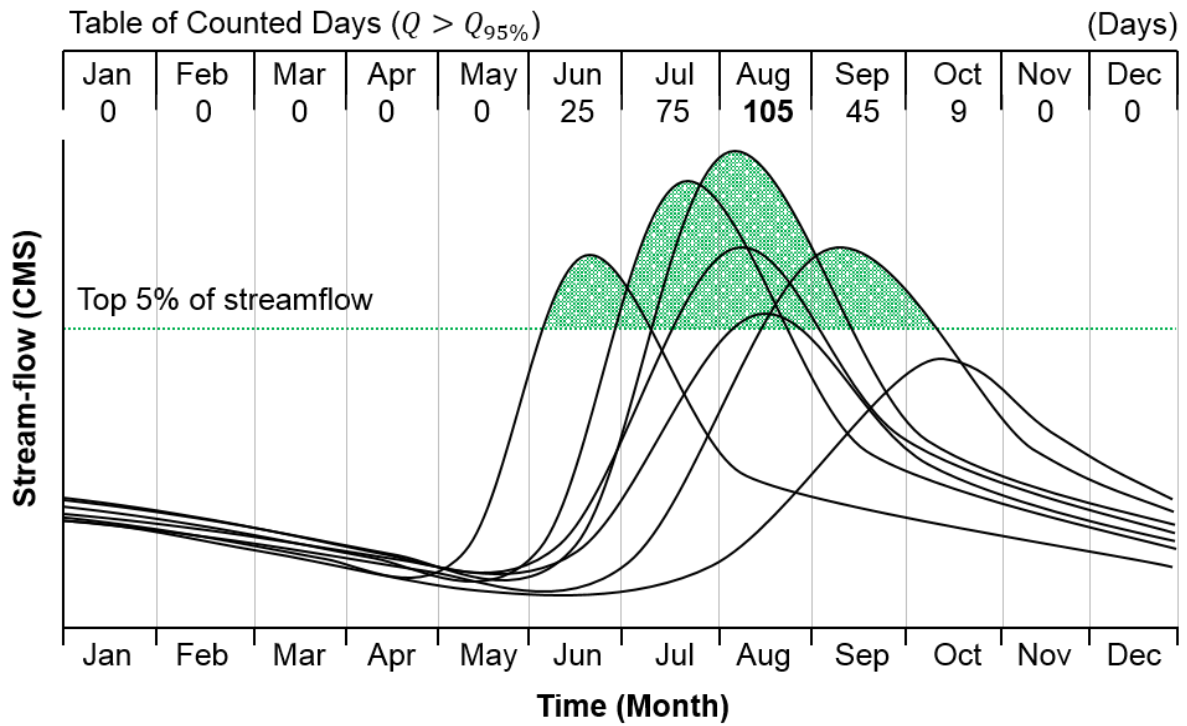
1 Table 4. Comparison of Peak Month (PM) for flooding and calculated  $P_{AMF}$  at 6 GRDC stations in the Zambezi River Basin.

Station (GRDC sta. numb.)	STA01 (1591001)		STA02 (1291100)		STA03 (1591406)		STA04 (1591404)		STA05 (1591403)		STA06 (1591401)		Final PM
Station name	Senanga		Katima Mulilo		Machiya Ferry		Kafue Hook Bridge		Itezhi-Tezhi		Kasaka		
River name	Zambezi		Zambezi		Kafue		Kafue		Kafue		Kafue		
Cumulative catchment area ( $km^2$ )	284,538		339,521		23,065		96,239		105,672		153,351		
Mean annual streamflow ( $m^3/s$ )	975		1168		139		287		353		988		
Streamflow type	Natural		Natural		Natural		Natural		Natural (Reservoir inflow)		Regulated		
Classification Technique	PM (month)	PAMF (%)	PM (month)	PAMF (%)	PM (month)	PAMF (%)	PM (month)	PAMF (%)	PM (month)	PAMF (%)	PM (month)	PAMF (%)	
Observed	4	96	4	100	3	93	3	100	3	94	7	36	3
Simulated	3	100	3	97	2	97	3	75	2	94	2	97	2

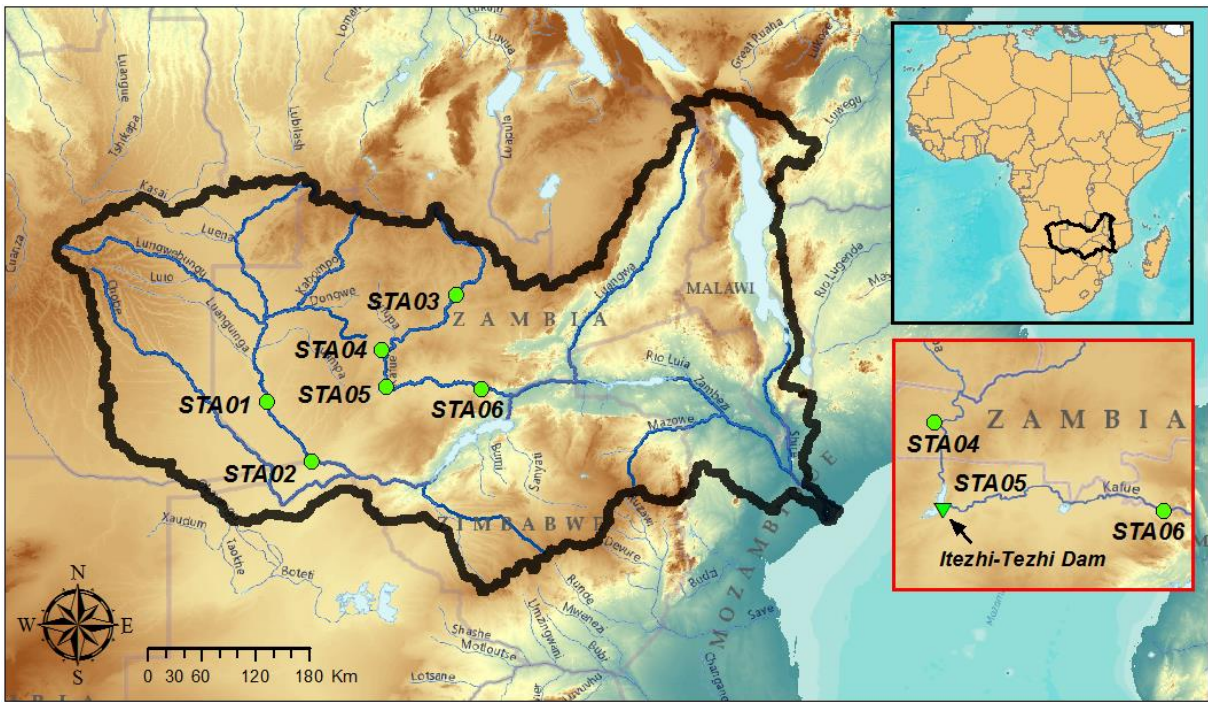
2



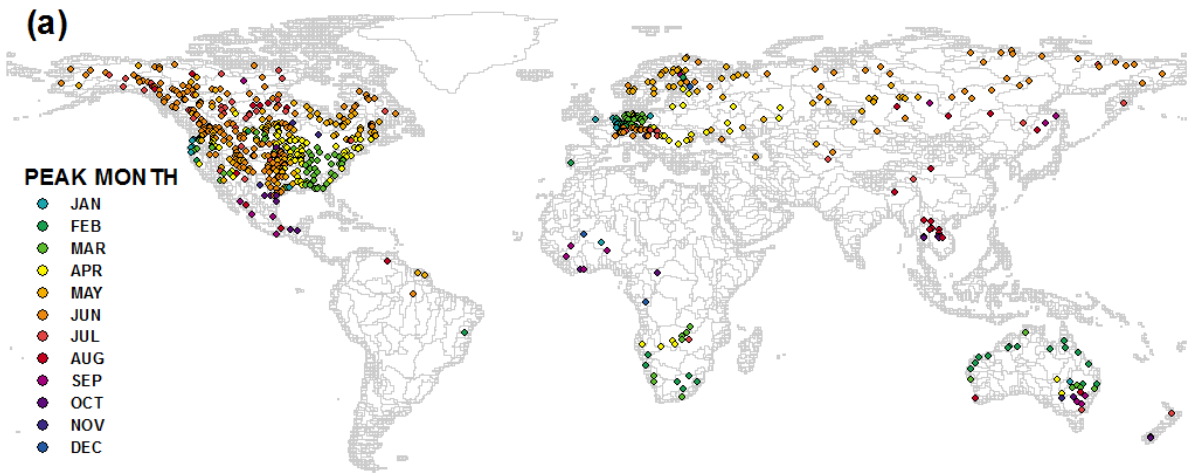
1  
2 Figure 1. Location of 691 selected GRDC stations with corresponding number of years per  
3 station. Background polygons are world sub-basins based on 30' drainage direction maps (Döll  
4 and Lehner, 2002) with separation of large basins (Ward et al., 2014).



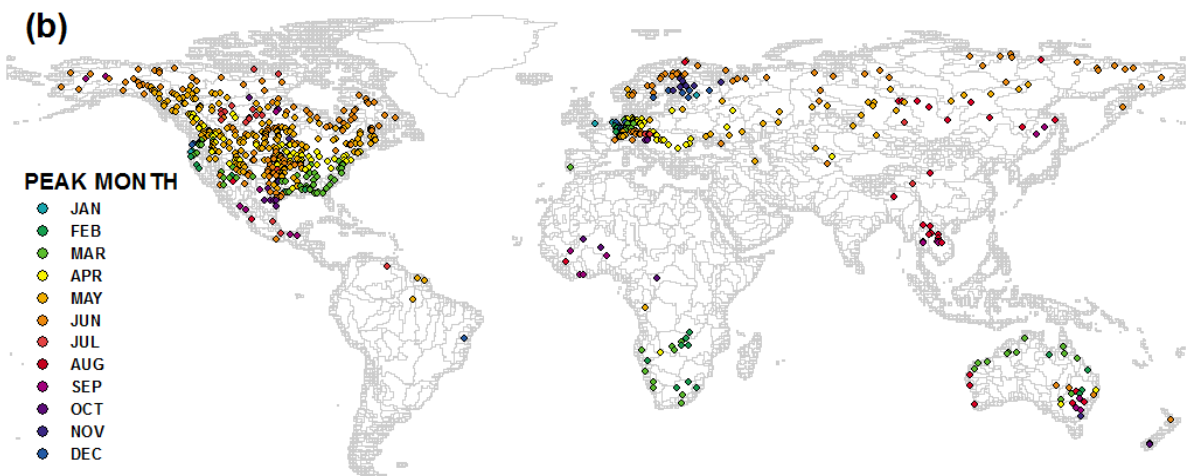
- 1
- 2 Figure 2. Seven years of synthetic streamflow data. Dotted line represents the 5% streamflow
- 3 threshold. Numbers indicates the total days above the threshold for each month.



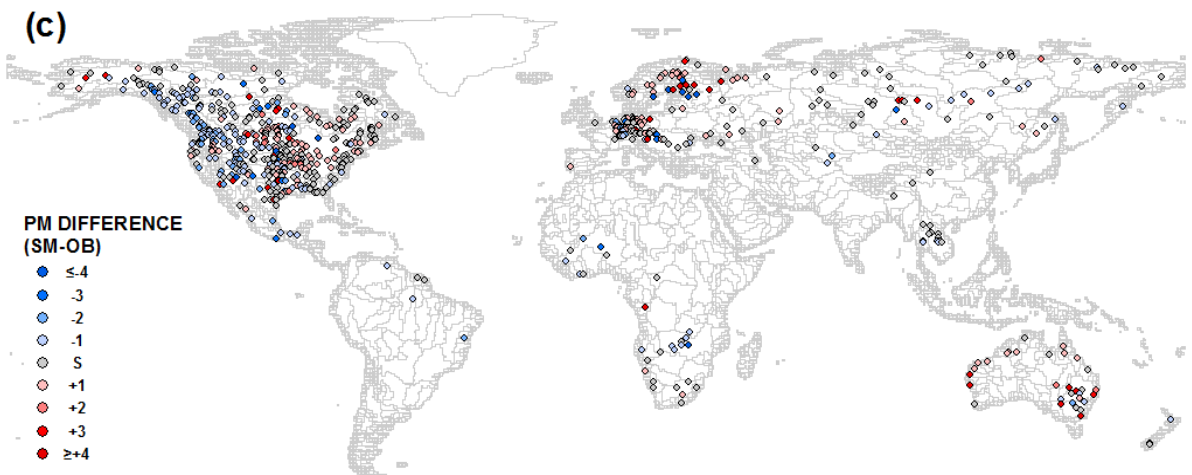
1  
 2 Figure 3. Map of Zambezi River Basin; the solid black line delineates the basin and the green  
 3 points are the 6 GRDC stations (STA01-06), with STA06 downstream of the Itezhi-Tezhi dam  
 4 (STA05→).



1



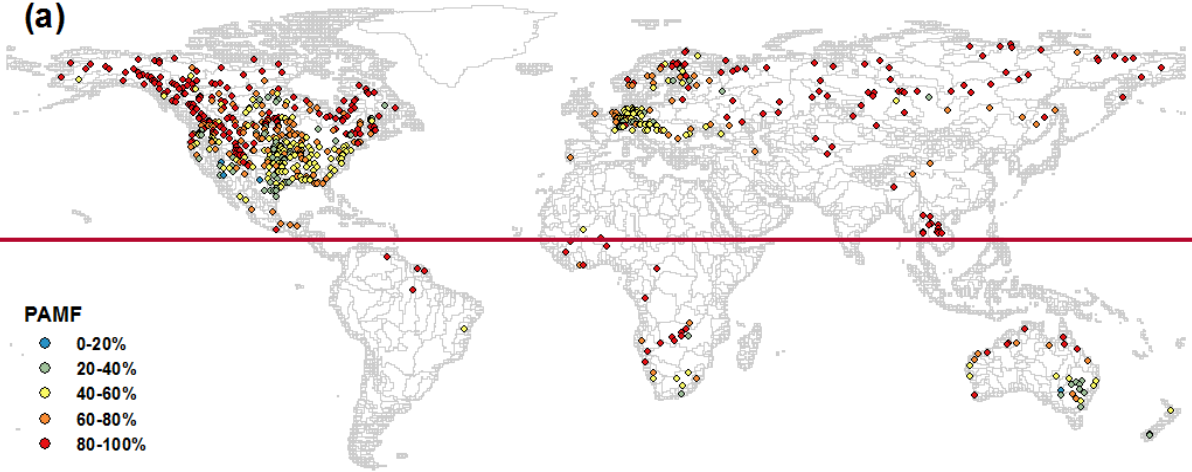
2



3

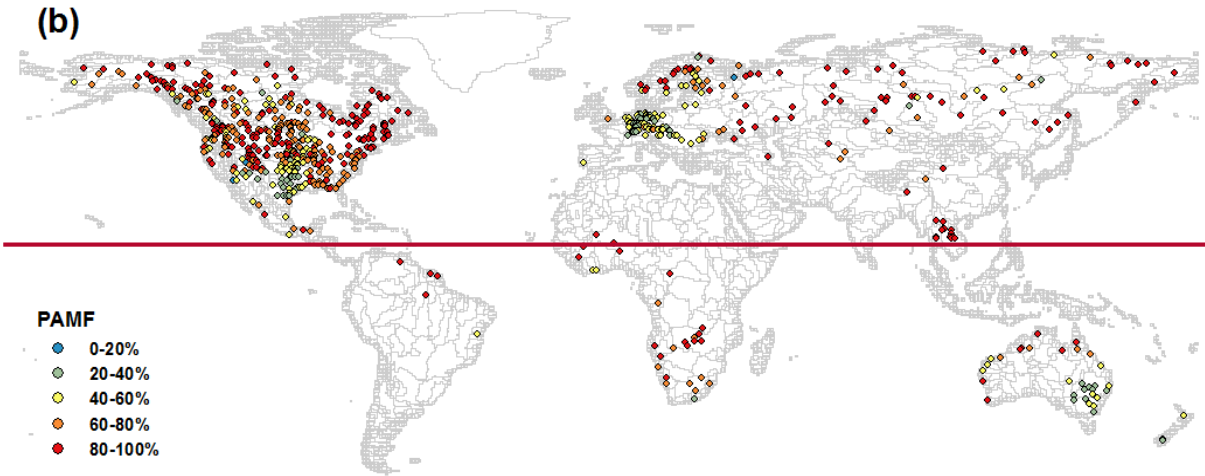
4 Figure 4. Peak Month (PM) for flooding as defined by (a) 691 GRDC observation stations, (b)  
 5 simulated streamflow at associated locations and (c) Temporal difference in PM between  
 6 observations and simulation (*SM-OB, number of months; Simulation-observation, in number of months;*  
 7 *negative (positive) value indicates that the simulated PM is earlier (later) than the observed*  
 8 *PM*).

(a)

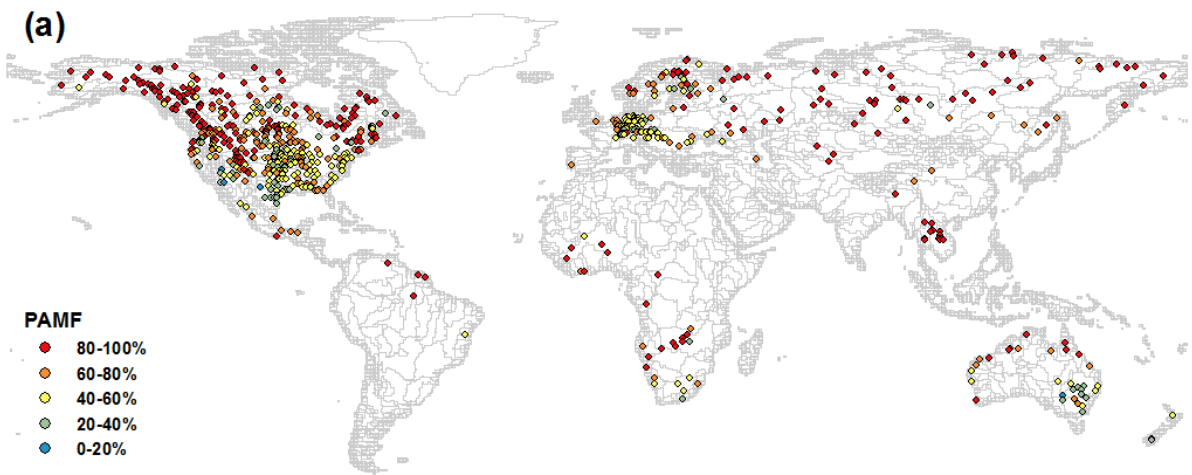


1

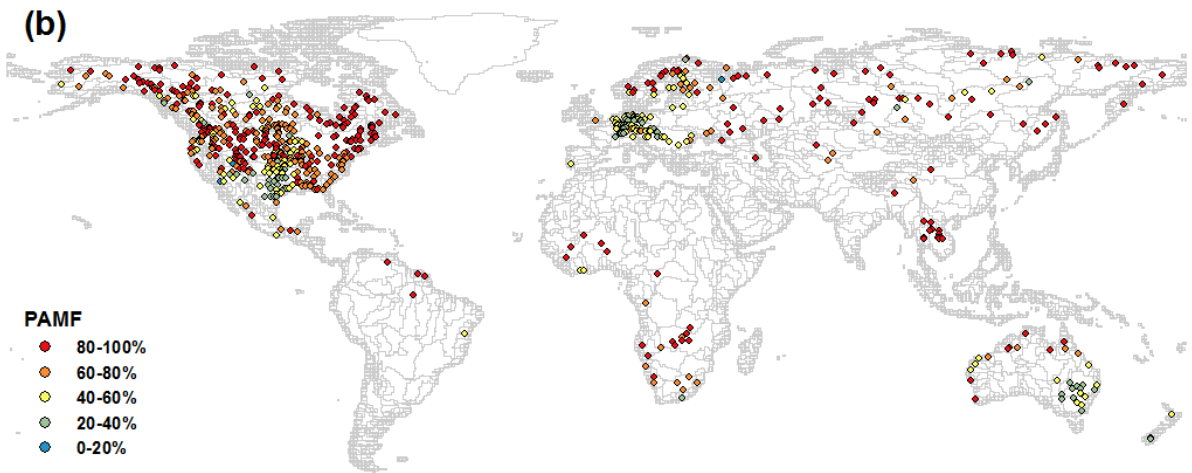
(b)



2



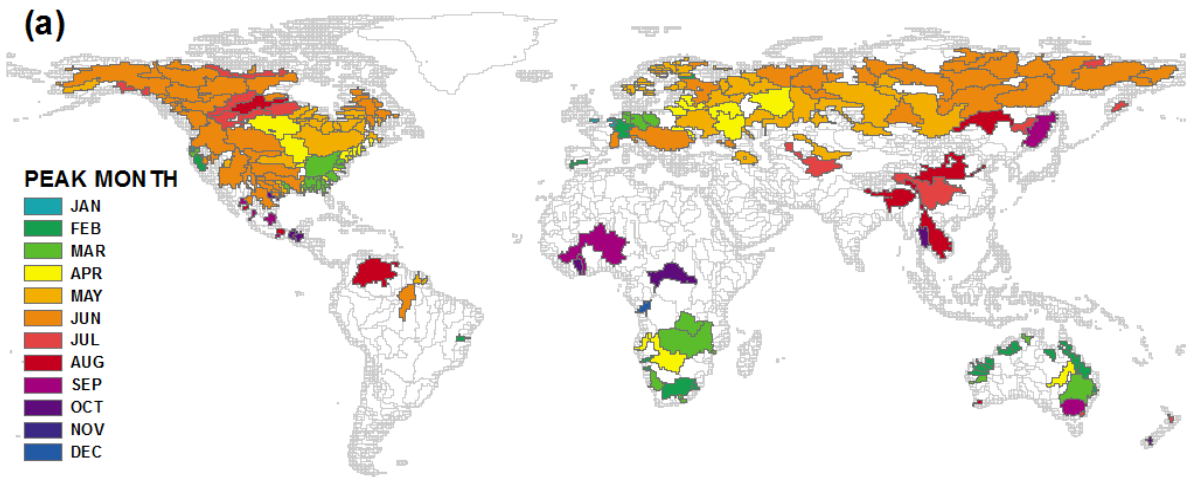
1



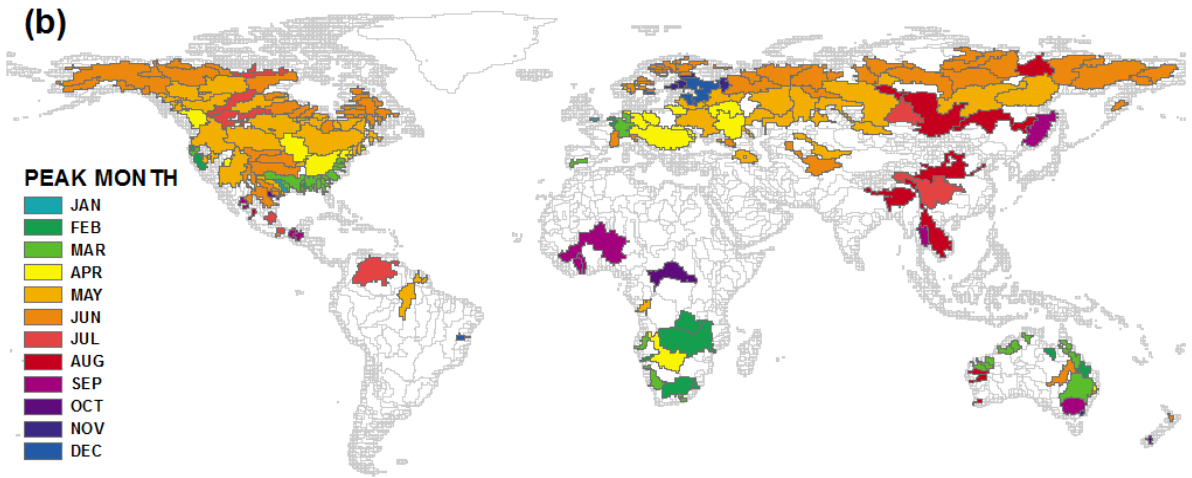
2

3 Figure 5. Calculated Percentage of Annual Maximum Flow (PAMF) values for (a) 691 GRDC  
 4 observation stations, and (b) simulated streamflow at associated locations: subjectively  
 5 classified as high = 80-100%, moderate = 60-80%, low = 40-60%, and poor = 0-40%.

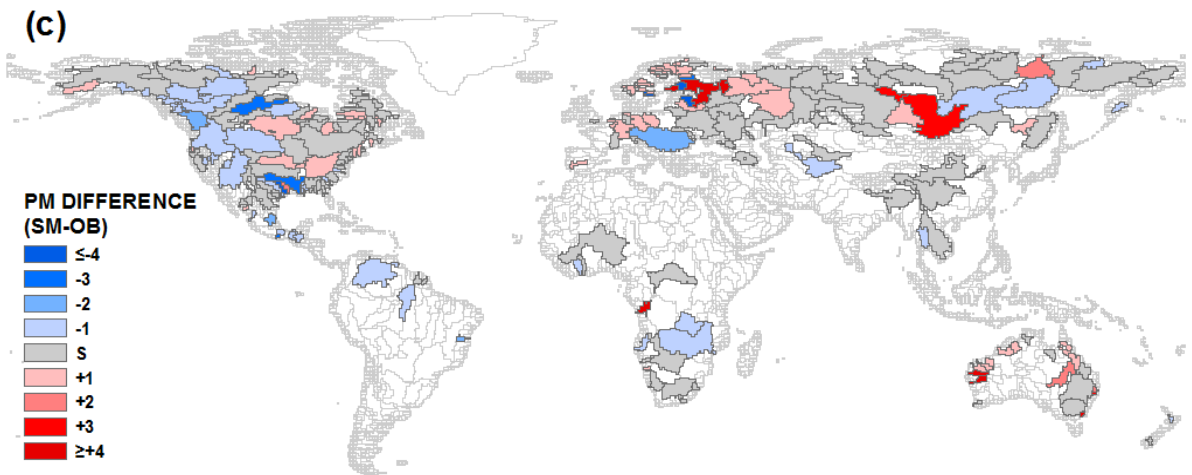




1



2



3

4

5

6

7

8

Figure 6. Peak Month (PM) for flooding by sub-basin as defined by (a) 691 GRDC observation stations, (b) simulated streamflow at associated sub-basins and (c) Temporal difference in PM between observations and simulation ( $SM-OB$ , number of months), simulation-observation, in number of months; negative (positive) value indicates that the simulated PM is earlier (later) than the observed PM).

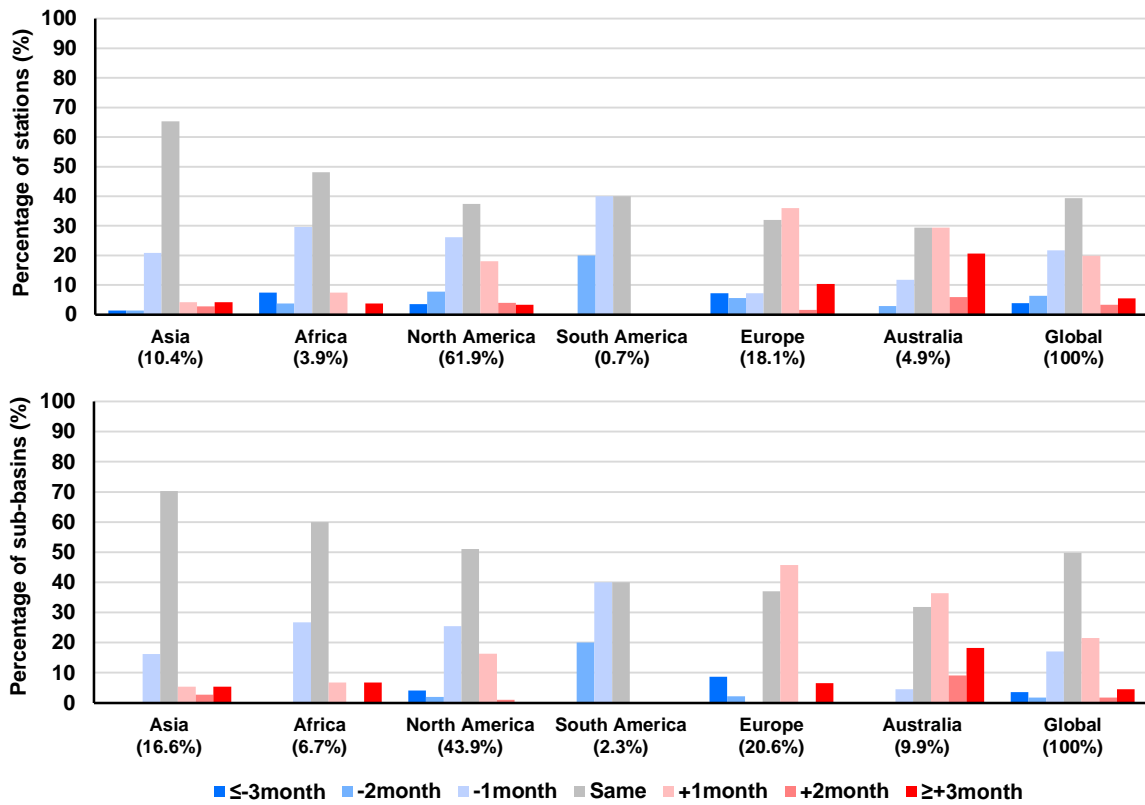
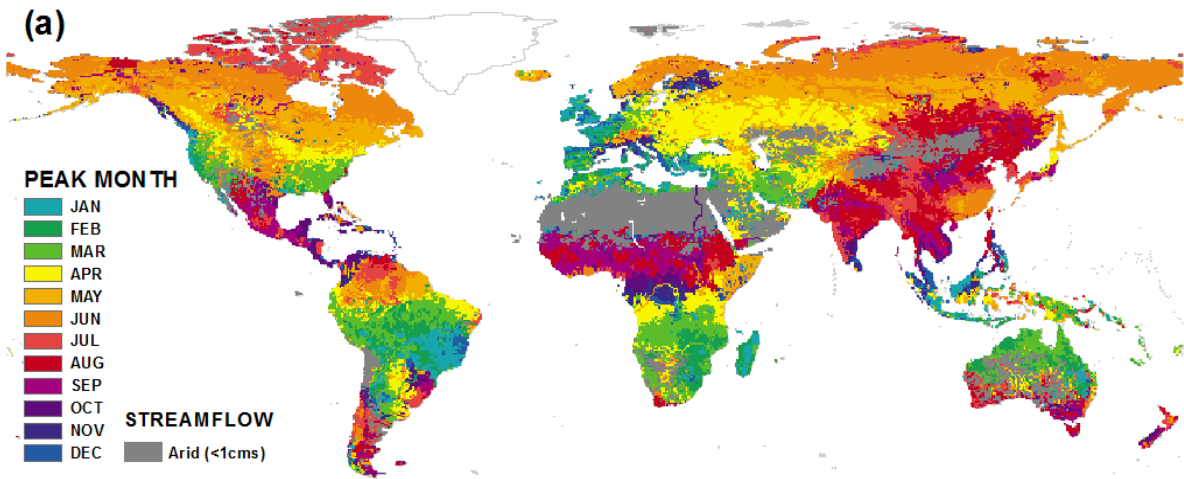
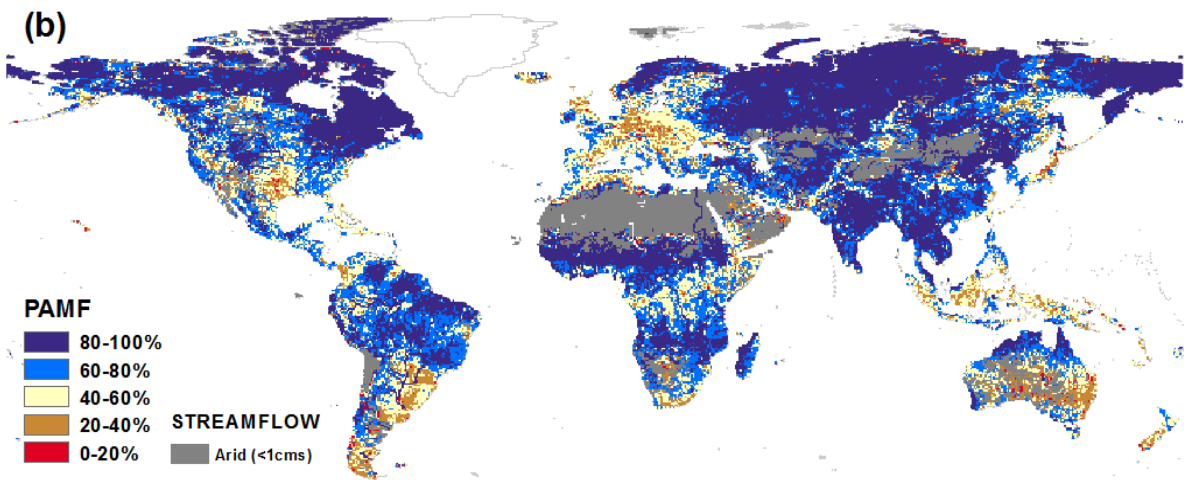


Figure 7. Percentage of stations (above) and sub-basins (below) according to temporal difference of PM between observations and model outputs (SM-OB, number of months) in each continent.



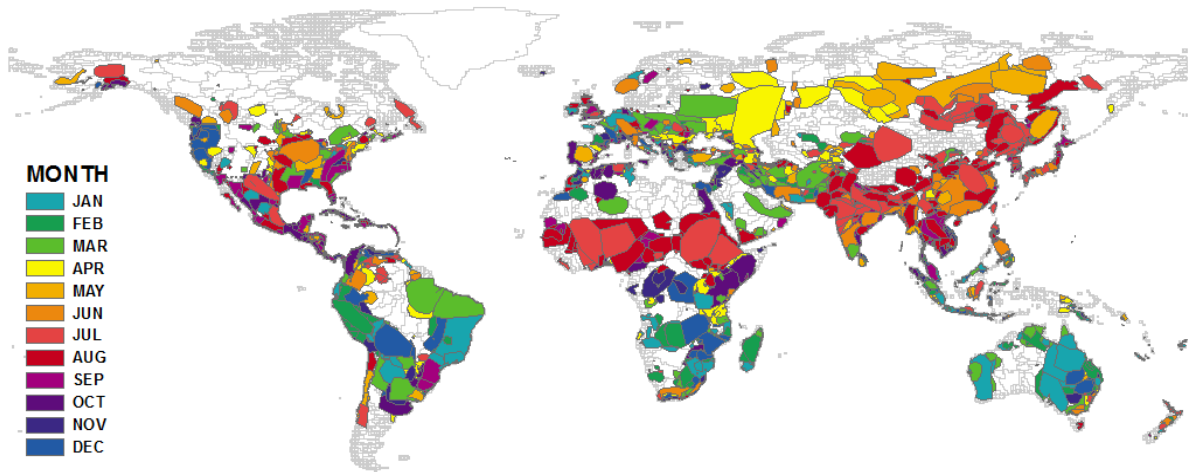
1



2

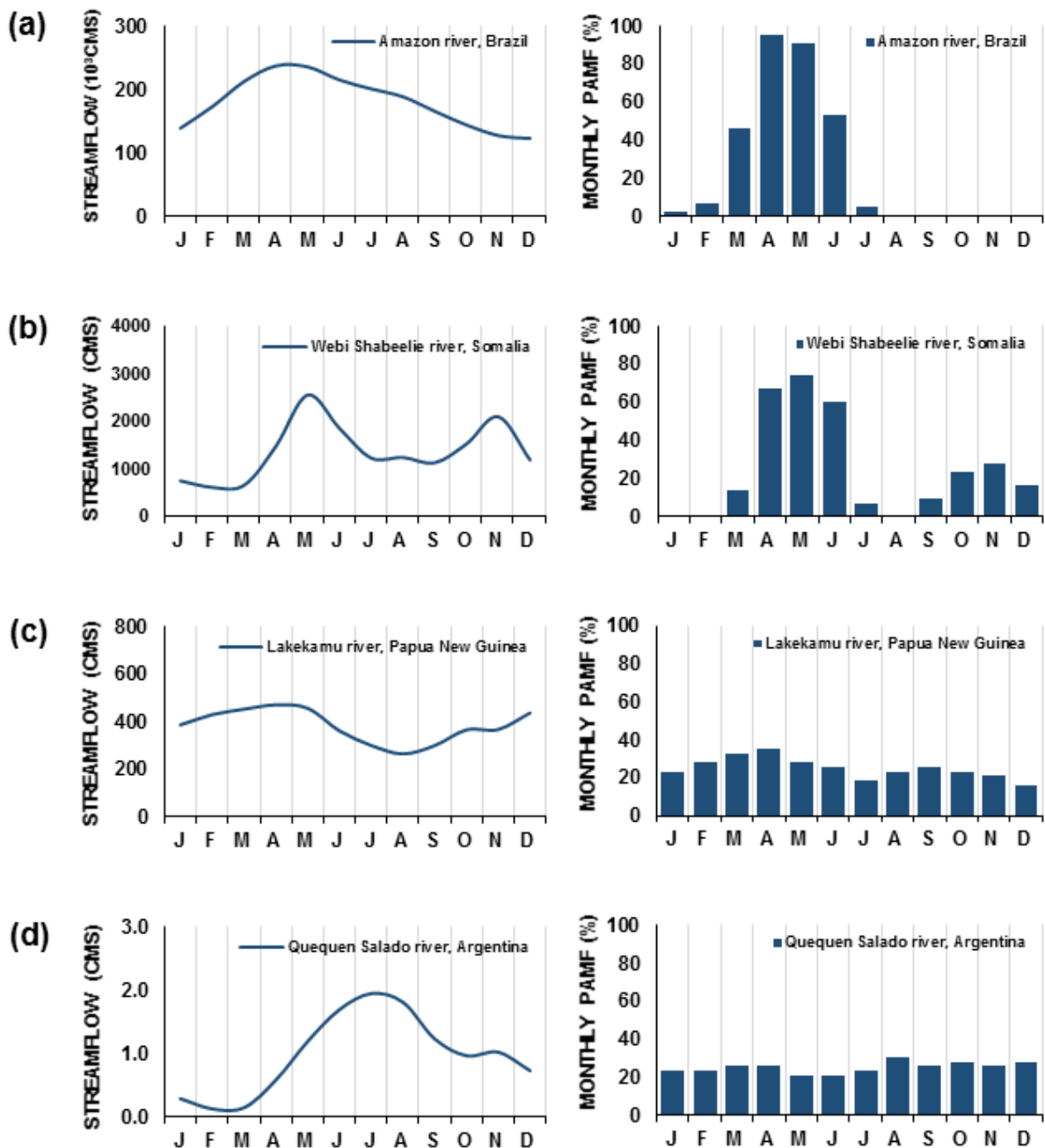
3 Figure 8. (a) Peak Month (PM) as defined at all modeled grid cells (b) Calculated Percentage  
 4 of Annual Maximum Flow (PAMF) values for at all modeled grid cells; subjectively classified  
 5 as high = 80-100%, moderate = 60-80%, low = 40-60% and poor = 0-40%.

6

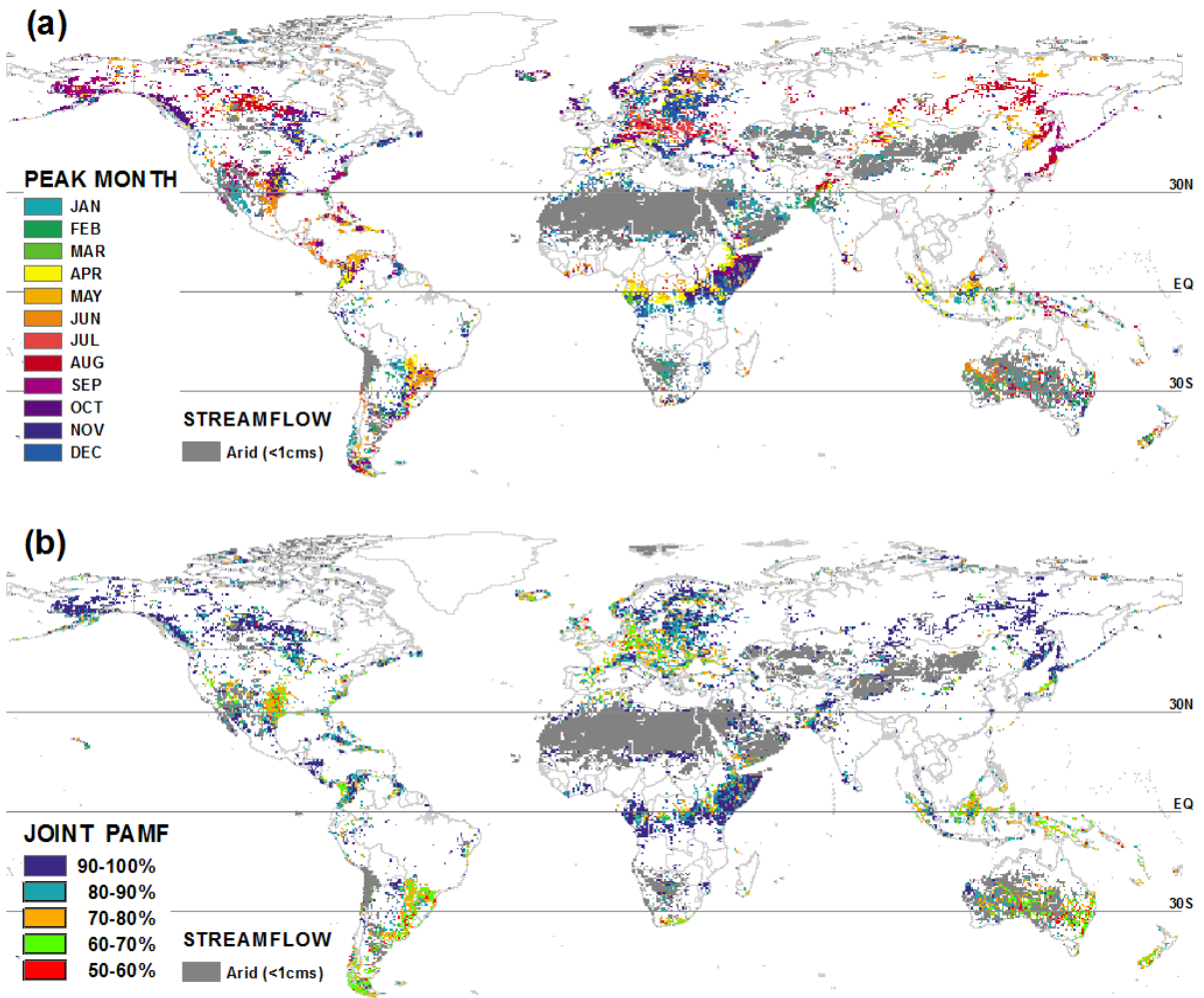


1

2 Figure 9. Archive of major flood events globally from the Dartmouth Flood Observatory (DFO) over 1985-  
 3 2008. Occurrence (start) months of 3,486 events from 'Global Active Archive of Large Flood  
 4 Events' from the Dartmouth Flood Observatory (DFO) over 1985-2008 (Brakenridge, 2011);  
 5 polygons indicate the estimated spatial extent, colors represent the start month, with most recent  
 6 events in time layered on top.



1  
2 Figure 10. Model-based streamflow climatology (left) and corresponding monthly PAMF  
3 (right). Types and locations are: a) uni-modal streamflow – At Bom Lugar, Amazon river,  
4 Brazil, b) bimodal streamflow – At Saacow, Webi Shabeelie river, Somalia, c) constant  
5 streamflow – At Terapo Mission, Lakekamu river, Papua New Guinea and d) low-flow – At La  
6 Sortija, Quequen Salado river, Argentina.



1

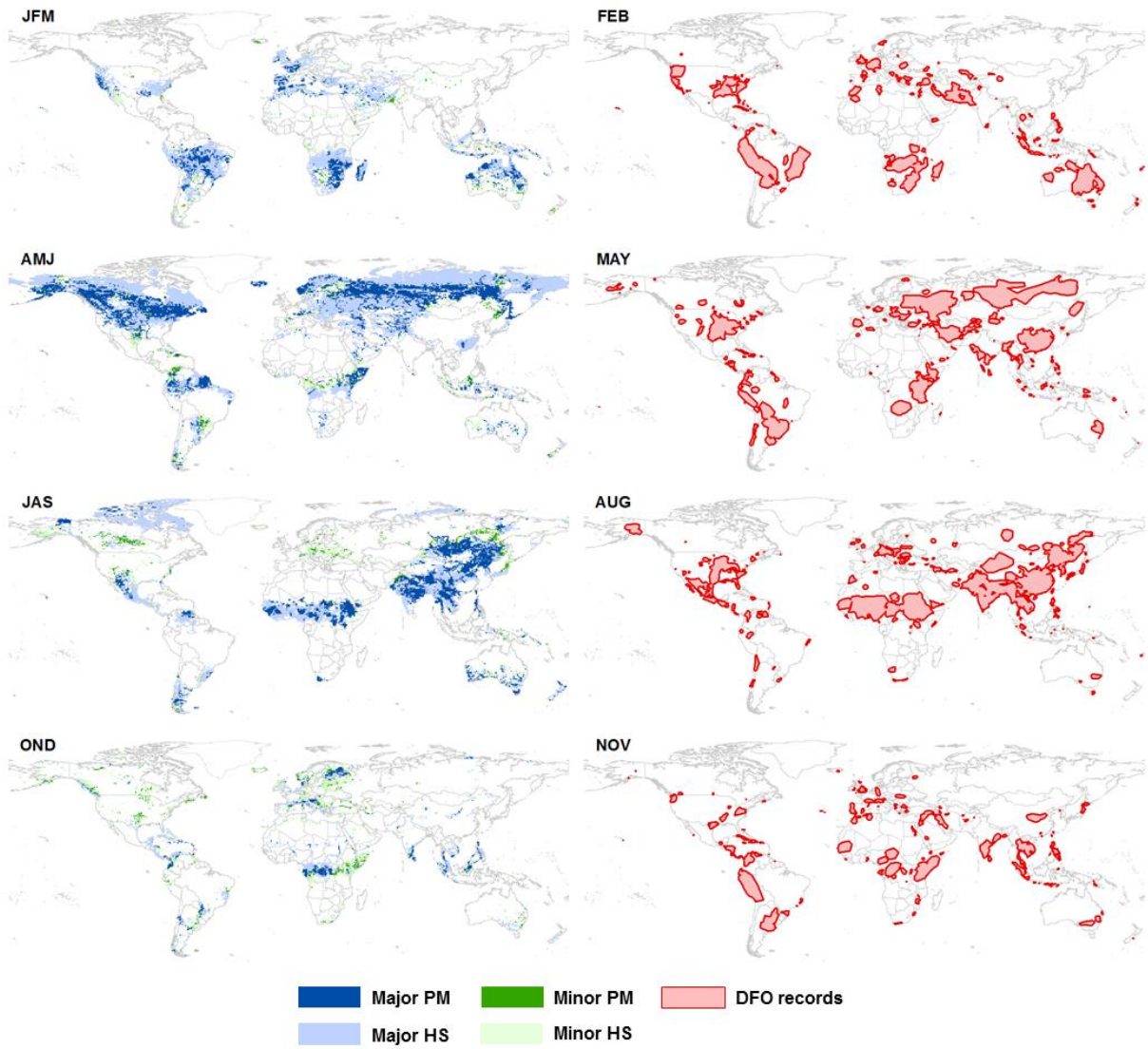
2

3

4

5

Figure 11. (a) Minor Peak Month (PM) for flooding as defined at detected grid cells and (b) joint PAMFs of major and minor PMs at corresponding cells; subjectively classified as high = 80-100%, moderate = 60-80%, and low = 40-60%.



1

2 Figure 12. Defined major HS and minor HS where joint PAMF is greater than 60% (left); peak  
 3 month of major and minor HSs (dense color) and pre- and post-month of major and minor HSs  
 4 (light color→). Monthly accumulated actual flood records (DFO) during 1958-2008 (right→).